TRANSIENT FLOW ANALYSIS OF FILLING IN PULSE DETONATION ENGINE

by

VEERA VENKATA SUNEEL JINNALA

Presented to the Faculty of the Graduate School of

The University of Texas at Arlington in Partial Fulfillment

of the Requirements

for the Degree of

MASTER OF SCIENCE IN AEROSPACE ENGENEERING

THE UNIVERSITY OF TEXAS AT ARLINGTON

December 2009

TO MY MOM, DAD, BROTHER AND FRIENDS

ACKNOWLEGEMENTS

I would like to gratefully acknowledge my advisor, Dr Frank K Lu, for being a constant source of guidance and inspiration. This work would not have been possible without his support and encouragement. I would like to thank Dr. Wilson, Dr. Stefan Dancila and Dr. Haji-Sheikh for agreeing to be on the defense committee, and reviewing my thesis.

Words are not enough to convey my gratitude to my colleagues, Philip Panicker, Richard Mitchell, Prashaanth Ravindran, Eric Braun and Albert Ortiz for all the helpful discussions, and times of fun inside and outside of Aerodynamic Research Center. I would like to acknowledge Santhosh VIjayshekar, Sanketh K and Hari Nagarajan for their guidance in Pro E and FLUENT.

I would like to thank my wonderful roommates, Raghu Ghandikota, Pavan R, Sampath Kotagiri, Amith Sivarai and Siddarth Kasyap for putting up with me and caring for me. My stay during this period at UTA would have been tough without Kishore Nekkanti, Uday Mallireddy, Deepak Bokka and Irshad Baig.I would like to thank Poornima Mynampati for her support.

Last but certainly not the least; I would like to thank Anupama Vadla for her friendship, support, motivation and encouragement for which I am indebted. I am grateful to her for helping me with MS Word for formatting my thesis report and all other help she extended to me during my days writing this work.

Finally, I am forever indebted to My Dad, Mom, and brother, for their love, constant motivation and encouragement throughout my education.

November 20, 2009

ABSTRACT

TRANSIENT FLOW ANALYSIS OF FILLING

IN PULSE DETONATION

ENGINE

Veera Venkata Suneel Jinnala, M.S

The University of Texas at Arlington, 2009

Supervising Professor: Frank K. Lu

The Pulse Detonation Engine (PDE) is considered to be a propulsion system of future air vehicles. The objective of the present study is to model an efficient inlet system for filling the detonation tube completely with the fuel/air mixture. In the present study the filling processes is modeled numerically using CFD code FLUENT^{TM}. Calculations for the gas flow are carried out by solving the Navier-Stokes equations coupled with the k- ε turbulence model.

Five different inlet configurations were proposed and simulated in both two-dimensionally and three-dimensionally. The model with an orifice plate at the inlets ensured the desired optimum results. The results of the simulation were discussed using velocity and pressure contours. The model developed could be a novel tool improving pulse detonation engine design.

TABLE OF CONTENTS

LIST OF ILLUSTRATIONS

Figure Page

LIST OF TABLES

CHAPTER 1

INTRODUCTION

1.1 Pulse Detonation Engine

Since the advent of the gas turbine engine, there has not been a major revolution in aircraft engine technology. Most chemical propulsion systems in use today rely on constant pressure combustion processes to convert chemical energy into useful thermal and kinetic energy as a means of generating thrust.[1] Compared to other current engine technologies, pulsed detonation engines (PDE) is one of a number of recent concepts that has the capability to offer mechanical simplicity, improved fuel efficiency, higher thrust-to-weight ratios, lower cost and a wide flight operation envelope.[2,3] For example, a comparison of specific impulse vs. Mach number regimes of various propulsion systems is shown in Figure1.1. This Figure clearly shows the superior propulsive performance of PDEs.

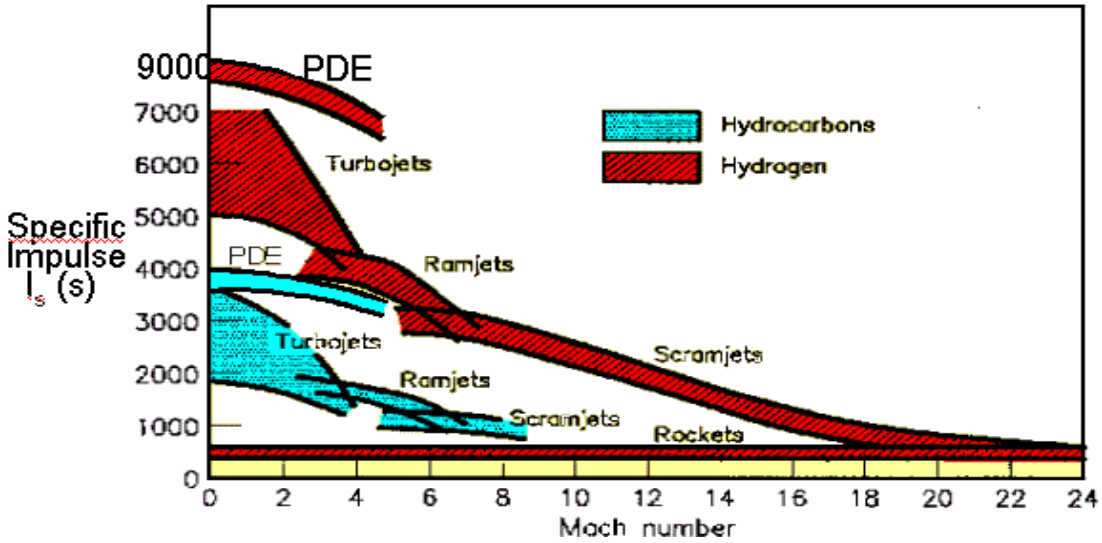

Figure 1.1 Specific Impulse vs. Mach number Regime of Various Propulsion Systems.[4]

Although early internal combustion engines all featured constant pressure deflagrative reactions, the benefits of constant volume combustion used to model detonations were well known to many pioneers in the propulsion arena. In 1941, H Hoffman, in Germany, tested a pulsed detonation engine prototype. Starting in the early 1990s, experimental study of single and multi combustor PDEs were conducted in many parts of the world.[6, 7, 8] Much of the current PDE studies are performed using CFD in order to comprehend and quantify the unsteady detonation phenomenon.

A PDE is a type of propulsion system that can potentially operate from subsonic up to hypersonic speeds.[9] Pulse detonation engines are simple in construction, light weight and produce large thrust. The PDE has a simple geometry, consisting of a tube which is filled with fuel and oxidizer. The PDE operates on the supersonic detonation of fuel. The basic block diagram of PDE is shown in the Figure 1.2.

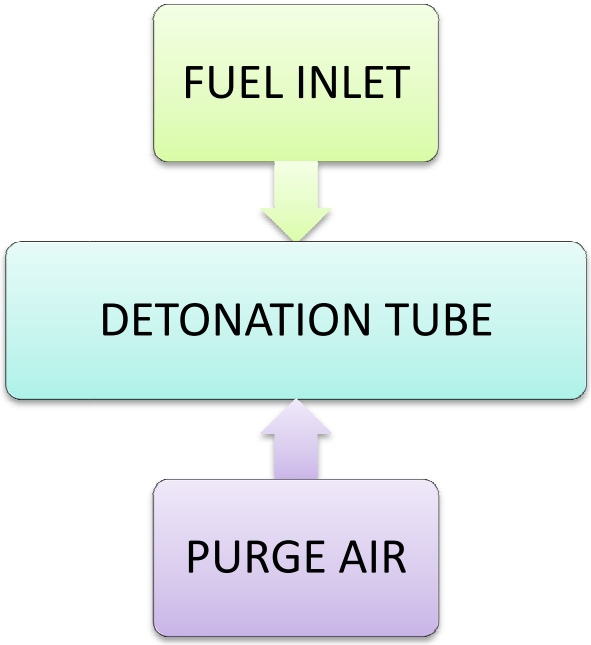

Figure 1.2 Block Diagram of a Pulse Detonation Engine

Such an engine does not require are frequently depicted as not to require compressors to, thereby reducing the overall weight and complexity of engine. The main difference between a pulse detonation engine and a traditional pulsejet is that the mixture does not undergo subsonic combustion but, instead supersonic combustion. The operational frequency of PDEs can range from a few tens to a few hundred cycles per second. The uninstalled thrust produced by the engine is a function of the number of detonation tubes, the cross-sectional area of each tube, frequency of operation and exit velocity of the exhaust gases.

Figure 1.3 outlines the various processes in pulse detonation cycle and described below.

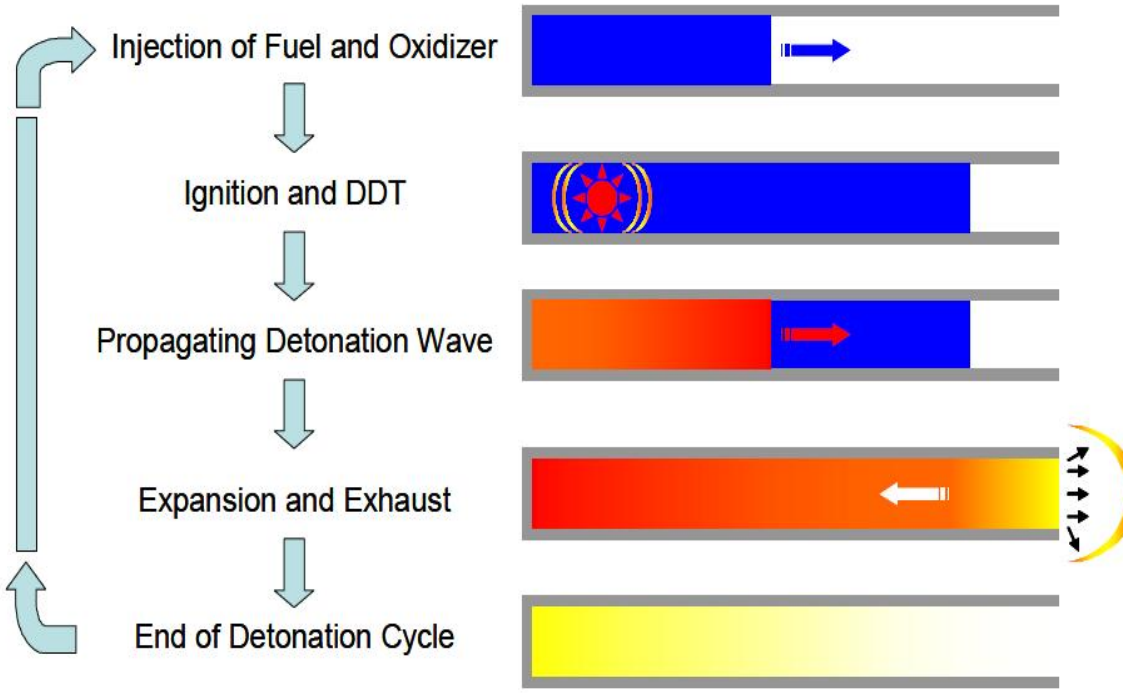

Figure 1.3 Schematic of a Pulse Detonation Engine Cycle.[5]

1.1.1 Filling Process

This process is to simply fill the detonation tube with fuel and oxidizer at a certain design mass flow rate or velocity. This process should be carried out very quickly, because any lengthening of the fill time will lead to a delayed detonation. In designing a PDE, the value used

for the filling velocity should be carefully assumed for achieving high flow rates and at the same time in ensuring acceptable flow losses. The time taken for the filling is denoted as t_{fill} .If x_L is the length of the detonation tube, then the filling time is calculated as,

$$t_{fill} = \frac{\text{length of the tube}}{\text{filling Velocity}} = \frac{x_L}{V_{fill}} \qquad (1.1)$$

where V_{fill} is the axial velocity with which the fuel and oxidizer mixture is pumped into the detonation tube.

1.1.2 Detonation Process

This process takes place after the filling process. In this process the detonation wave is created which moves through the mixture and causes the pressure and temperature behind it to rapidly shoot up. Compared with the filling process, detonation takes place at a fraction of a millisecond. The velocity with which the detonation wave travels from the closed end to the open end is termed the detonation velocity. The time taken for the detonation wave to take shape and to move through to the end of the combustion chamber is denoted by t_C . The Chapman-Jouguet velocity is the velocity that an ideal detonation travels at as determined by the Chapman-Jouguet (CJ) condition: the burned gas at the end of the reaction zone travel at sound speed relative to the detonation wave front. CJ velocities can be computed by solving for thermodynamic equilibrium and satisfying mass, momentum, and energy conservation for a steadily-propagating wave terminating in a sonic point. CJ velocities in typical fuel-air mixtures are between 1400 and 1800 m/s.

The detonation time of this wave is calculated as

$$t_c = \frac{\text{length of the tube}}{\text{CJ wave Velocity}} = \frac{x_L}{D_{cj}} \qquad (1.2)$$

1.1.3 Rarefaction or Blowdown Process

In this process a series of unsteady rarefaction waves travel upstream into the combustion chamber and reflects off the end wall, causing high-pressure burnt gasses to exit the combustion chamber. The values of the thermodynamic properties of the rarefaction wave are smaller when compared with those of the detonation-wave. The time taken by the rarefaction wave in traveling through the detonation tube will be much higher than that of the detonation wave because the velocity of the rarefaction wave is less than that of the detonation. The time taken for the blowdown stage is denoted by t_b and is calculated as follows.

$$t_b = \frac{\text{length of the tube}}{\text{rarefaction velocity}} = \frac{4x_L}{D_{cj}} \qquad (1.3)$$

The greater time period of this process plays a major role in cooling the tube after the detonation process.

1.1.4 Purging Process

This is the final process in a pulse detonation cycle. Fresh air is blown through to clean and cool the tube before the fill stage starts again. The time taken for this process is calculated along the same lines as the filling process. The higher the purge velocity, the lower the purge time and ultimately, the faster the cycle times. The purging process is very important as this cools the tube and prevents the fresh fuel /oxidizer mixture from auto-igniting .The time taken for purging the tube with fresh air is given by

$$t_{purge} = \frac{\text{length of the tube}}{\text{purging Velocity}} = \frac{x_L}{V_{purge}} \qquad (1.4)$$

The total time period T of one cycle is the sum of all time for the four stages,

$$T = t_{fill} + t_c + t_b + t_{purge} \qquad (1.5)$$

The frequency of operation f is the inverse of the time period. Thus reducing the period increases the operational frequency. As been highlighted, the filling and purging processes take a larger fraction of the period.

1.2 Objective of Current Research

The focus of the FLUENT simulation is to ensure a smooth flow of the reactants through the detonation tube in a short time and without any dead air regions and isolated pockets of residual gas. A very important improvement that can be made to a PDE is to shorten the fill time.

The objective of the current work is to design an efficient inlet system for filling the detonation tube completely with the fuel/air mixture. The filling process should be carried out very quickly, because any lengthening of the fill will delay subsequent stages of the PDE cycle. For the current work, sidewall injection was chosen to accomplish the filling process as otherwise the injection from the closed end will take more time to completely fill the detonation tube. The sidewall injection system will have inlets throughout the length of the detonation tube at regular intervals, where as in closed end injection we have only one inlet. As the fuel enters from a number of inlets in sidewall injection, this will also help in reducing the dead air regions and the isolated pockets of residual gas etc. The results were summarized to explain the benefits of sidewall injection.

CHAPTER 2

METHODOLOGY

FLUENT™ was employed in the present work. It uses a finite volume scheme to solve the continuity, momentum and energy equations with the associated boundary conditions. In any CFD simulation, the first step is to model the geometry and generate the mesh. In this work, Pro E™ was used to create the geometry and GAMBIT™ was used for meshing the geometry. The mesh file was then imported into FLUENT™, where the modeling equations and boundary conditions are set.

2.1 Pro/Engineer™ Model

A generic CAD model of a potential PDE configuration was drawn in Pro E™. The PDE consists of a detonation tube at the center. Detonation tube has an internal diameter of 101.6 mm and a length of 1000 mm. On one side of it is a fuel/air mixture chamber and on the other side is a purge air chamber. These chambers are connected to the detonation tube by two rotary valves, see Figure 2.1.

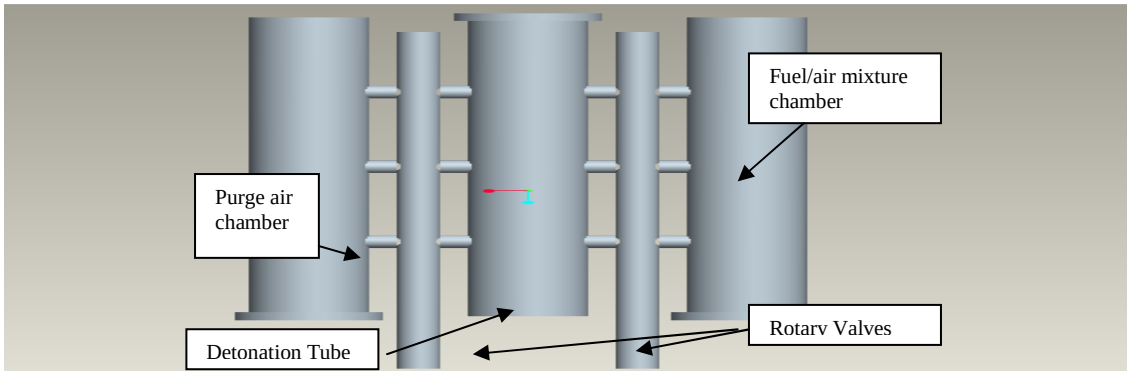

Figure 2.1 CAD Schematic is Showing the Top View of Important PDE Components.

In an actual engine, each rotary valve is connected to stepper motors, which controls the opening and closing of the rotary valve at regular intervals.

Further, additional geometry was removed to isolate the problem of gas injection. Figure.2.2 shows one of the configurations of the simplified model, which consists of only the detonation tube with eight side injection ports and an end injection port at the closed end.

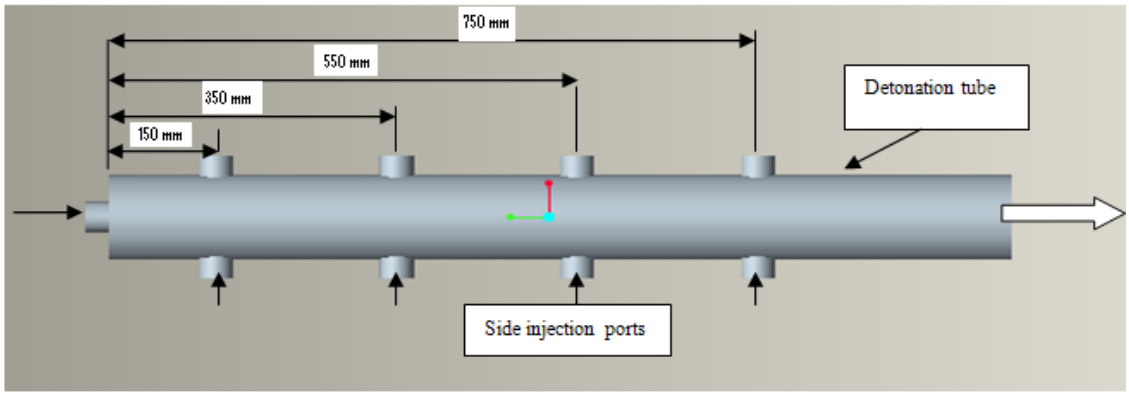

Figure 2.2 Top View of Final Simplified Model of Detonation Tube.

Five different injection schemes were studied. The five configurations are end wall injection, oppositely offset inlets, diametrically opposite flow inlets with and without inlet at the closed end, and inlet with an orifice plate. The dimensions of the final simplified model are listed in Table 2.1

Table 2.1 Dimensions of the Detonation Tube

Length	1000 mm
Internal Diameter	101.6 mm
Injection Port Diameter	25.4 mm
Thickness	6.35 mm

2.2 Meshing

The model shown in Figure.2.2 is imported from Pro E™ to GAMBIT™. GAMBIT™ was used to distribute tetrahedral meshes for 3-D models. Figure 2.3 (a-d) shows the mesh distribution of all the five 2-D configurations. The dimensions of all the models are identical as displayed in Table 2.1.

A model with end wall injection was designed for capturing the filling of the detonation tube with the reactants. For accomplishing the objective of the present work to fill the detonation tube completely, the initial design was modified by increasing the number of injection ports as shown in Figures 2.3(a-e). Finally, an orifice plate is added to the inlets for filling the detonation tube more effectively.

Initially, five two-dimensional cases were studied and these were then extended to three-dimensional models. A denser mesh near the inlet walls is adopted to capture the propagation of reactants entering the detonation tube more accurately.

Table 2.2 below shows the number of cells, faces and nodes for all the four configurations.

Table 2.2 Two Dimensional Configurations Mesh Details

Case	Cells	Faces	Nodes
Case i	5800	11855	5920
Case ii	5506	11275	5776
Case iii	6267	12850	6584
Case iv	18300	37040	18741
Case v	25759	40852	20096

(a)

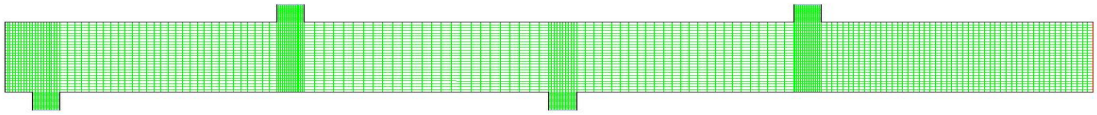

(b)

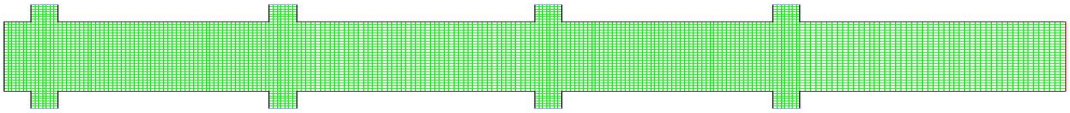

(c)

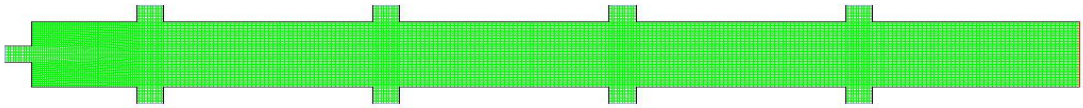

(d)

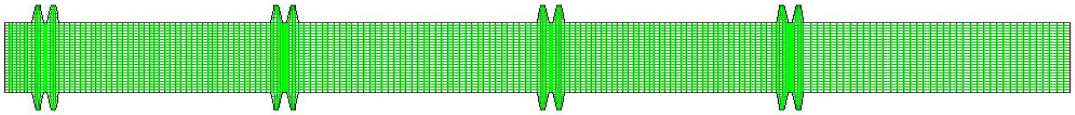

(e)

Figure 2.3 Two Dimensional Cases Studied Showing Mesh Distribution (a) Case i: mesh for model with end wall injection, (b) Case ii: mesh for model with oppositely offset inlets, (c) Case iii: mesh for the model with diametrically opposite flow inlets, (d) Case iv: mesh for the model with a inlet at the closed end, (e) Case v: mesh for the model with orifice plate in the inlets.

In three-dimensional models a fine mesh was used at the edges in order to resolve the steep gradients near the walls. Figures 2.5 (a-e) shows the mesh distribution of the three- dimensional models. In case 5, with an orifice plate at the inlet shape functions[12] are used at the intersection of the orifice plate and the detonation tube inlet as shown in Figure 2.5 (e). The smallest node size used for meshing is 0.5 mm and the largest node size is 2 mm. Detailed meshing of the orifice plate is shown in Figure 2.5 (e). Even in places of less interest, a fine mesh was used since a coarse mesh may not yield good results. The detailed geometry of the orifice plate is shown in Figure 2.4.The holes in the orifice plate are set at 30 degrees angle, each hole is 3 mm in diameter. The diameter and thickness of the orifice plate is 25.4 mm 3.18 mm respectively.

The final pre-processing in GAMBIT™ included adding boundary conditions such as the wall, outlets and inlets.

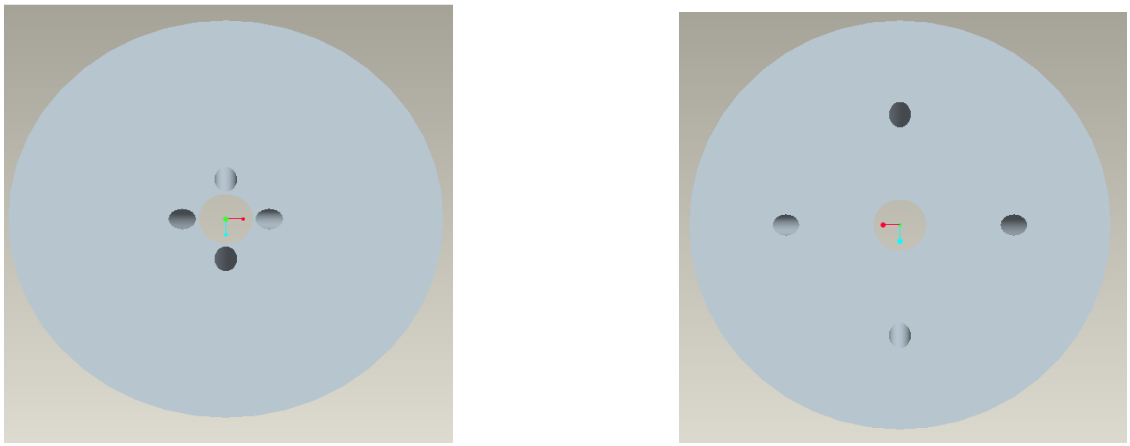

(a) (b)

Figure 2.4 Orifice Plate Design, (a) top view, (b) bottom view.

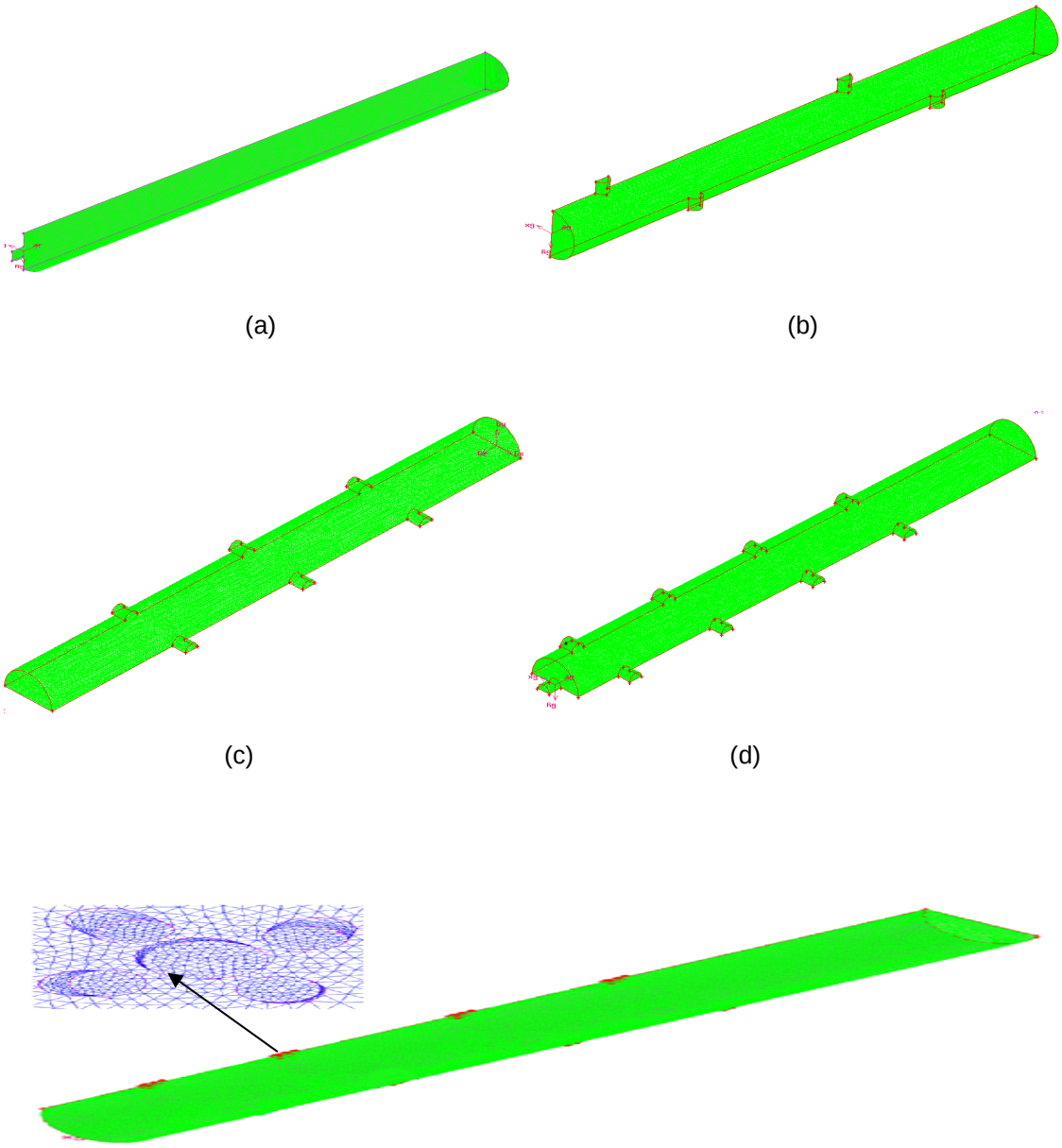

Figure 2.5 Three Dimensional Isometric Views of Cases Studied Showing Mesh Distribution (a) Case 1: mesh for model with end wall injection, (b) Case 2: mesh for model with oppositely offset inlets, (c) Case 3: mesh for the model with opposite flow inlets, (d) Case 4: mesh for the model with a inlet at the closed end, (e) Case 5: mesh for the model with orifice plate in the inlets.

Table 2.3 provides the mesh details pertaining to three dimensional configurations,

Table 2.3 Three Dimensional Configurations Mesh Details

Case	Cells	Faces	Nodes
Case 1	305126	681156	65933
Case 2	405126	841739	78793
Case 3	936985	1916156	175126
Case 4	949992	1929918	176188
Case 5	1506642	2038088	197344

2.3 FLUENT™

An important step in the set up of the model is to identify the fluid which in this case is air. Air is acceptable as a surrogate for a fuel /air mixture as there is no combustion taking place during the filling processes. The properties of air or a fuel/air mixture remain unaffected during the filling processes.

2.3.1 Solution Method

The SIMPLEC finite volume method was used to solve the partial differential equations of the model[13]. An unsteady solver was chosen to capture the propagation of the reactants entering the PDE during the filling stage. The segregated solution algorithm was selected to solve the governing equations. Double precision was used to alleviate error associated with the high aspect ratio grid. In addition to applying the material properties of the fluid, boundary conditions must be applied. For simplicity and as a first step in investigating the turbulence effects for the current research work the most simple k- ε model with default settings is preferred.

The inlet boundary condition of the model was set as mass flow ($\dot{m}$ = 0.288 kg/s). The direction of the flow was normal to the inlet boundary. And the outlet was specified as pressure out. So the outlet boundary is 1 atm. Each time step was determined and monitored by the solver. Additional details and a more exact set up of the boundary conditions are supplied in Appendix (A).Finally in order to start the analysis time step size (Dt) is required. Time step size is calculated as follows:

$$D\,t = \frac{d\,x}{V} \tag{2.1}$$

Where dx is cell size, V is the velocity.

2.3.2 Governing Equations

The given problem is solved using the above mentioned initial conditions, boundary conditions and a turbulence model, using the Navier-Stokes equations. The general form of conservation equations, neglecting the body force is given.[10]

Continuity $$\frac{\partial(\rho)}{\partial t} + div(\rho V) = 0 \tag{2.2}$$

x-momentum $$\frac{\partial(\rho u)}{\partial t} + div(\rho u V) = -\frac{\partial p}{\partial x} + div(\mu\ grad(u)) \tag{2.3}$$

y-momentum $$\frac{\partial(\rho v)}{\partial t} + div(\rho v V) = -\frac{\partial p}{\partial y} + div(\mu\ grad(v)) \tag{2.4}$$

z-momentum $$\frac{\partial(\rho w)}{\partial t} + div(\rho w V) = -\frac{\partial p}{\partial z} + div(\mu\ grad(w)) \tag{2.5}$$

Energy $$\frac{\partial(\rho e)}{\partial t} + div(\rho e V) = -div(V) + div\big(k\ grad(T)\big) + \emptyset \tag{2.6}$$

where ρ is the density, μ is the dynamic viscosity, T is the temperature and Φ is the dissipation function. The two-dimensional form of the equation can be obtained by dropping the parameters relevant to third dimension.

The realizable k-ε model is defined by the following two transport equations, one for the turbulent kinetic energy (k) and second for the rate of dissipation of turbulent kinetic energy (ε).[11]

$$\frac{\partial}{\partial t}(\rho k)+\frac{\partial}{\partial x_i}(\rho k u_i)=\frac{\partial}{\partial x_j}\left[\left(\mu+\frac{\mu_t}{\sigma_k}\right)\frac{\partial k}{\partial x_j}\right]+G_k+G_b-\rho\varepsilon-Y_M+S_k \qquad (2.7)$$

$$\frac{\partial}{\partial t}(\rho \varepsilon)+\frac{\partial}{\partial x_i}(\rho \varepsilon u_i)=\frac{\partial}{\partial x_j}\left[\left(\mu+\frac{\mu_t}{\sigma\varepsilon}\right)\frac{\partial \varepsilon}{\partial x_j}\right]+C_{1\varepsilon}\frac{\varepsilon}{k_M}\left(G_k+C_{3\varepsilon}G_b\right)-C_{2\varepsilon}\rho\frac{\varepsilon^2}{k}+S_\varepsilon \qquad (2.8)$$

In these equations, G_k represents the generation of turbulence kinetic energy due to the mean velocity gradients; G_b is the generation of turbulence kinetic energy due to the buoyancy; Y_M represents the contribution of the fluctuating dilatation in compressible turbulence to the overall dissipation rate; $C_{1\varepsilon}, C_{2\varepsilon}$ and $C_{3\varepsilon}$ are constants; and σ_k and σ_ε are the turbulent Prandtl numbers for k and ε, respectively. The values of the constants can be listed as:

$C_{1\varepsilon}$=1.44, $C_{2\varepsilon}$=1.92, C_μ=0.09, σ_k=1.0, σ_ε=1.3

These default values have been determined from experiments with air and water for fundamental turbulent shear flows including homogenous shear flows and decaying isotropic

grid turbulence. They have been found to work fairly well for a wide range of wall – bounded and free shear flows.

CHAPTER 3

RESULTS AND DISCUSSION

3.1 Description of Results

The pulse detonation engine model, governing equations of the flow inside the detonation tube and numerical solution methods were introduced in previous chapters. The investigation considered the propagation of reactants into the detonation tube, during the filling process. Both two- and three- dimensional (2-D and 3-D) cases, developed in chapter 2, are studied. Isometric views of pressure and velocity contours and velocity and pressure contours of the two-dimensional model are grouped together respectively for each case. As mentioned in chapter 2 five different configurations are analyzed in FLUENT^{TM}. In the figures velocities are presented in m/s and the pressures are presented in Pa.

3.1.1 Convergence

Convergence is checked for the velocity components, continuity and energy in all the four cases. Convergence is determined by checking the scaled residuals and ensuring that they are less than 10^{-3} for all variables except for the energy equation in which the residuals have to be less than 10^{-6}. The model is considered as converged when the velocity, continuity and energy approach constant values. Figures 3.1-3.4, display the trend of the residuals in the velocity, continuity, energy, TKE, and dissipation with the number of iterations in two-dimensional models.The *x* axis represents number of iterations, while *y* axis represents the residual value.

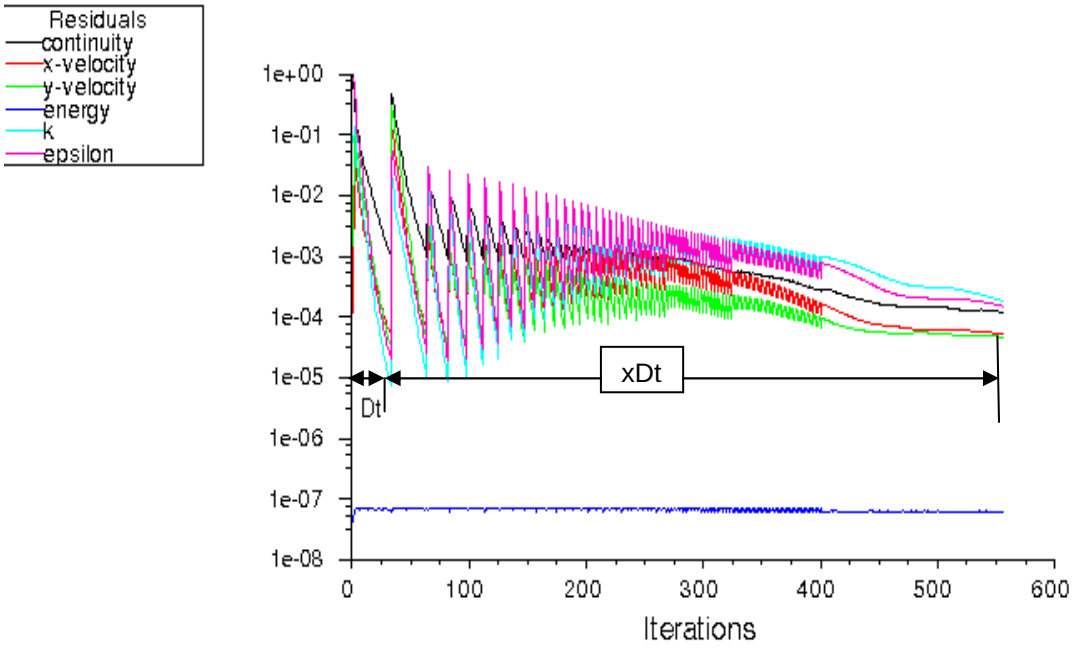

Figure 3.1 (Case i) Residual Plots of Model with End Wall Injection.

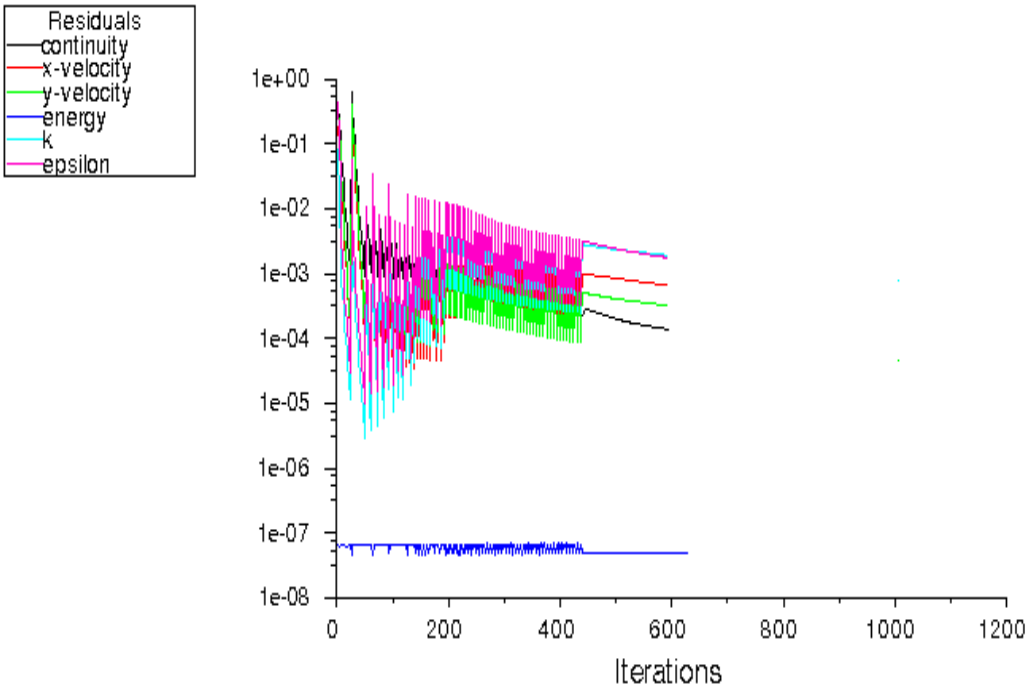

Figure 3.2 (Case ii) Residual Plots of Model with Offset Inlets.

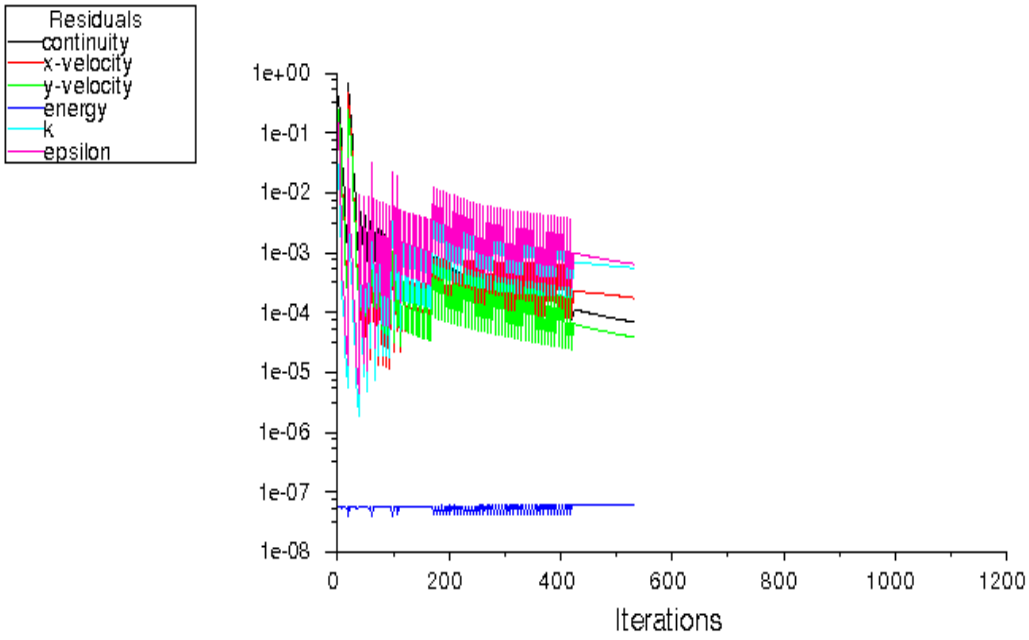

Figure 3.3 (Case iii) Residual Plots of Model with Opposite Inlets.

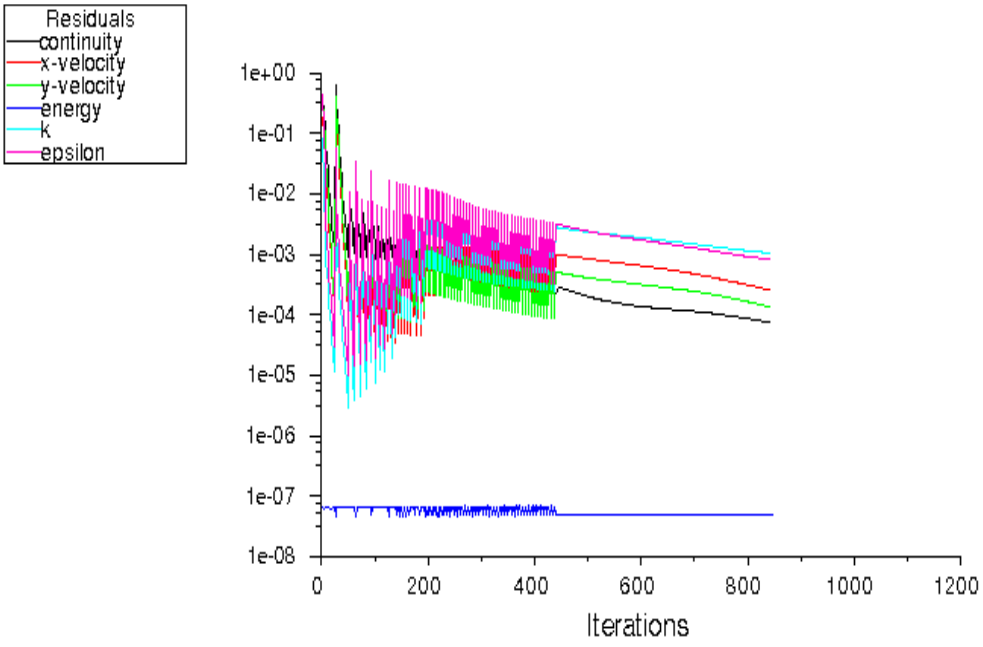

Figure3.4 (Case iv) Residual Plots of Model with Inlet at the Closed End.

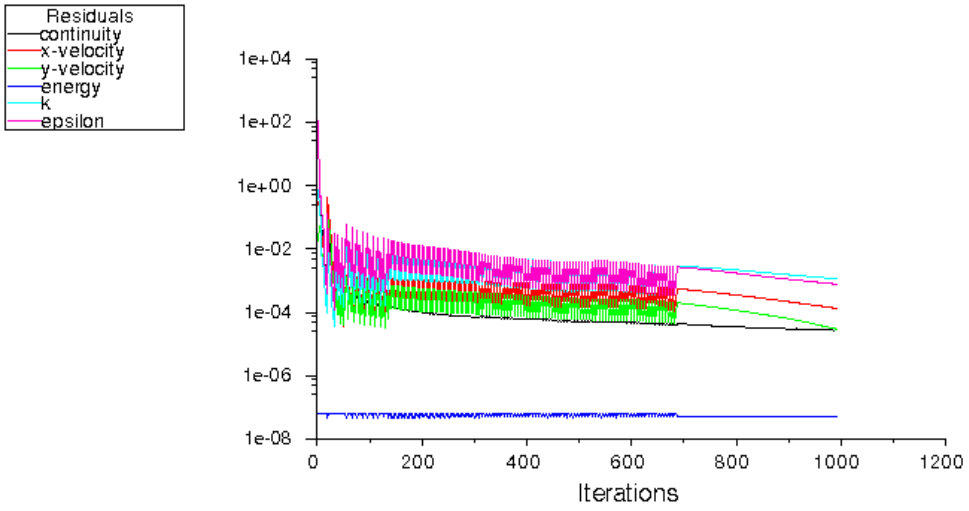

Figure 3.5 (Case v) Residual Plots of Model with Orifice Plate in the Inlets.

Table 3.1 furnishes the number of iterations needed for convergence in all the five cases along with the grid size in use. The convergence was concluded based on the observation of the trends of salient properties viz., continuity, velocity components, energy, TKE and dissipation.

Table 3.1 Details of Iterations and Grid Size of 3D Models.

Cases	No. of Iterations	Cells
Case 1	580	5800
Case 2	640	5506
Case 3	540	6267
Case 4	880	18300
Case 5	1000	25759

It is seen that the number of iterations depends on the size of the grids and number of cells. For case 5, the number of iterations was comparatively more than the remaining cases, because of the finer mesh (see chapter 2). Also, it can be observed that the convergence was obtained with a much higher order of accuracy in case 5 than other cases. Similarly convergence for three-dimensional models is also checked.

3.1.2 Case 1

The following velocity and pressure contours show the propagation of reactants in the detonation tube during the filling processes in the model with end wall injection. The contour level serves as a visual aid that indicates the propagation of reactants inside the detonation tube. This model is the existing PDE design.

The velocity contours in Figure 3.8 shows that detonation tube is partially filled with a very low velocity. Thus increasing the filling time. Figure 3.6 shows the velocity and pressure contours of two dimensional model. Figures 3.7 and 3.8 shows the velocity and pressure contours at t =0.08 s and t =0.2 s iterations respectively.The time taken to fill the detonation tube $t_{fill} = 0.2$ s.

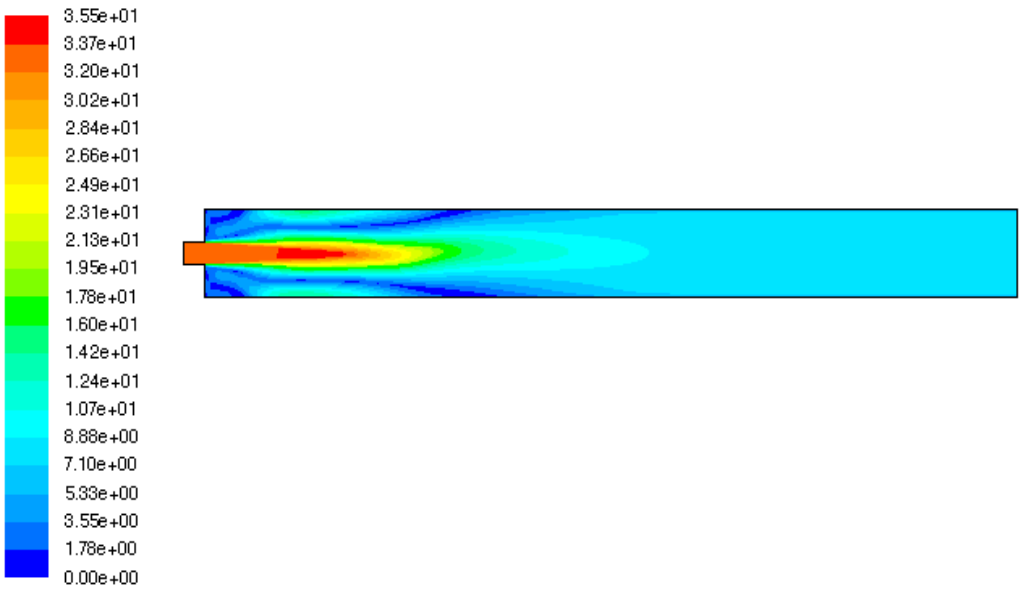

(a)

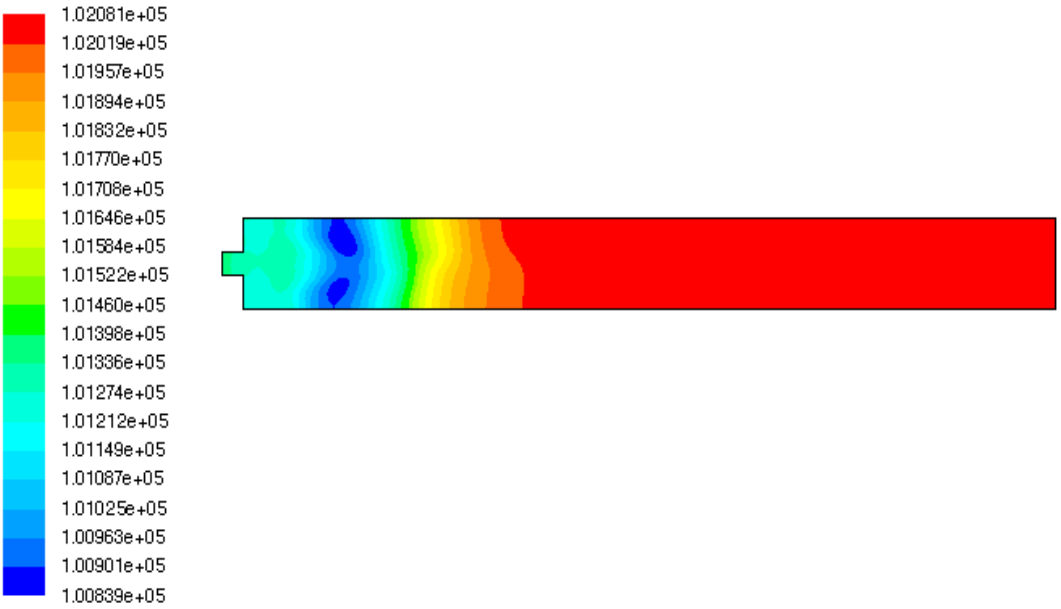

(b)

Figure 3.6 Velocity and Pressure Contours of Two-dimensional Model with End Wall Injection at t =0.2 s, (a) Case i: 2-D velocity contours, (b) Case i: 2-D pressure contours.

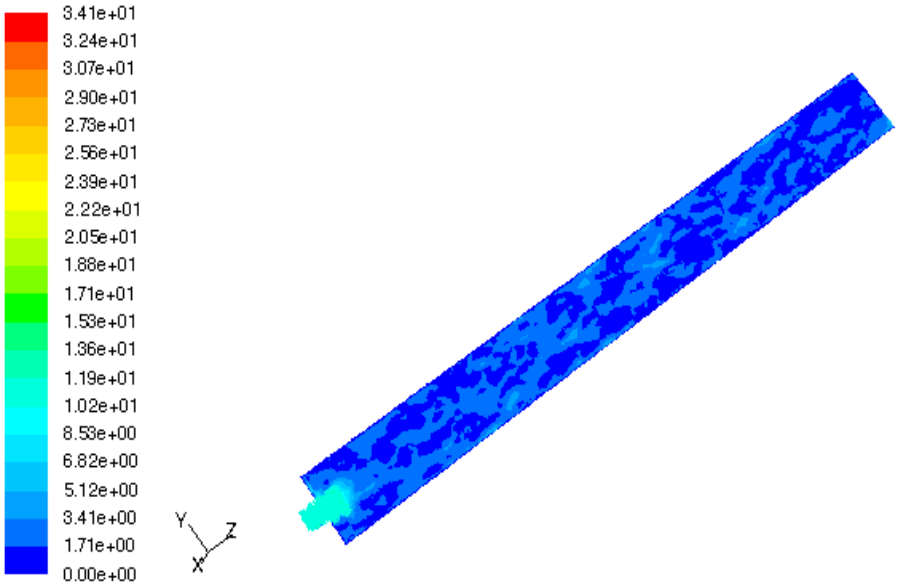

(a)

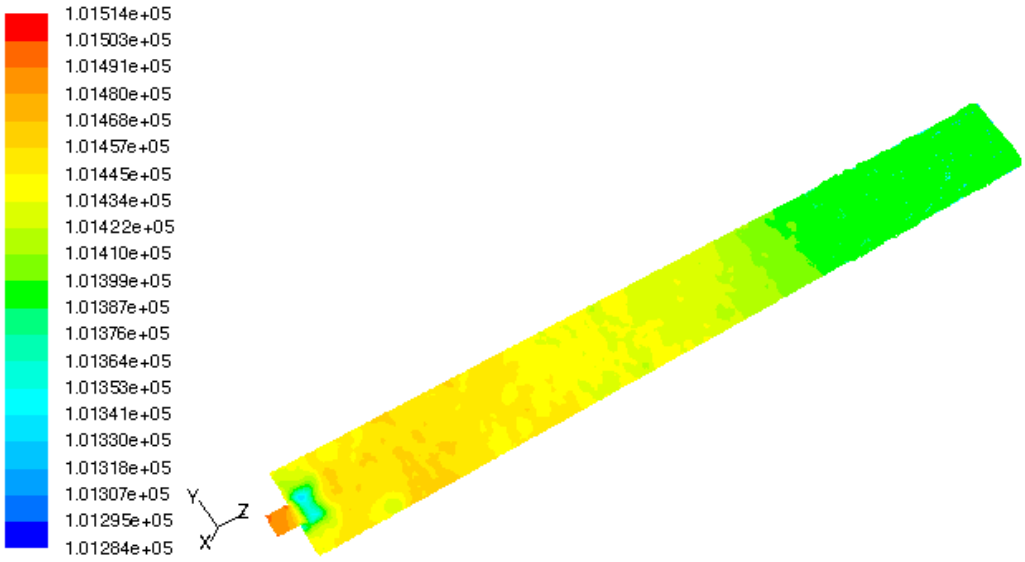

(b)

Figure 3.7 Isometric Views of Velocity and Pressure Contours at t =0.08 s, (a) Case 1: 3-D velocity contours, (b) Case 1: 3-D pressure contours.

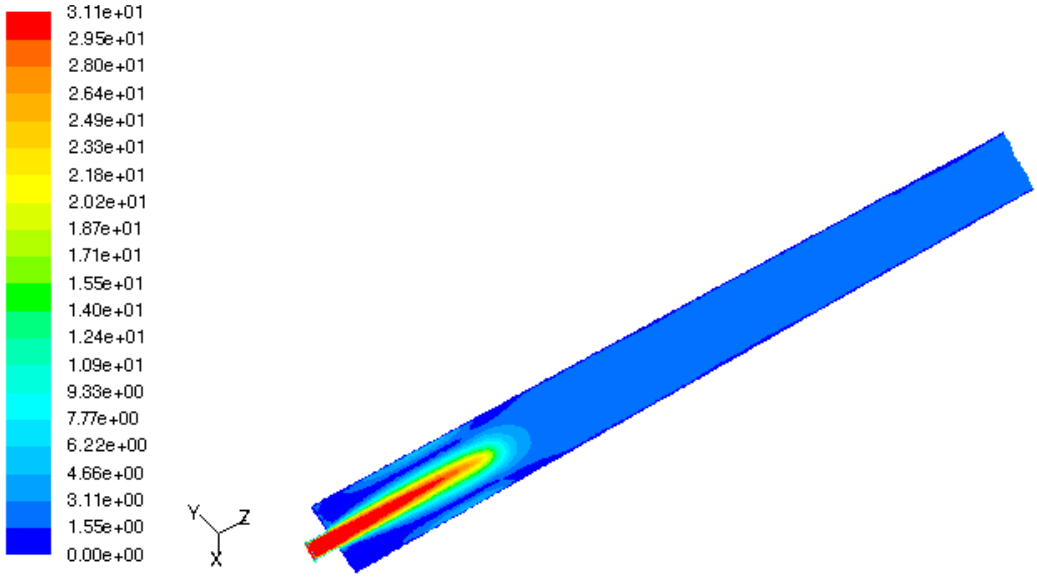

(a)

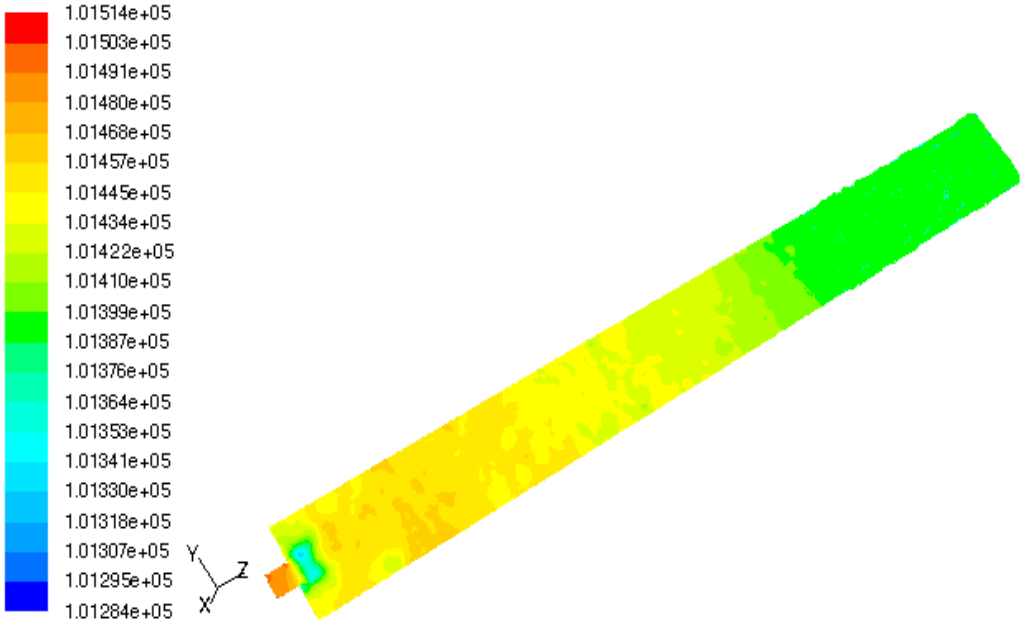

(b)

Figure 3.8 Isometric Views of Velocity and Pressure Contours at t =0.2 s (a) Case 1: 3-D velocity contours, (b) Case 1: 3-D pressure contours.

3.1.3 Case 2

The velocity contours presented in Figures 3.10-3.11 show that the detonation tube is not completely filled with reactants as some dead air regions are spotted. The dead air regions are those where nil velocity prevails, see Figure 3.11 (a). Figures 3.10 and 3.11 shows the velocity and pressure contours at t =0.001 s and t =0.01 s iterations respectively.The reactants in the detonation tube flows from left to right. The velocity inside the detonation tube ranges from 0 to 31 m/s.

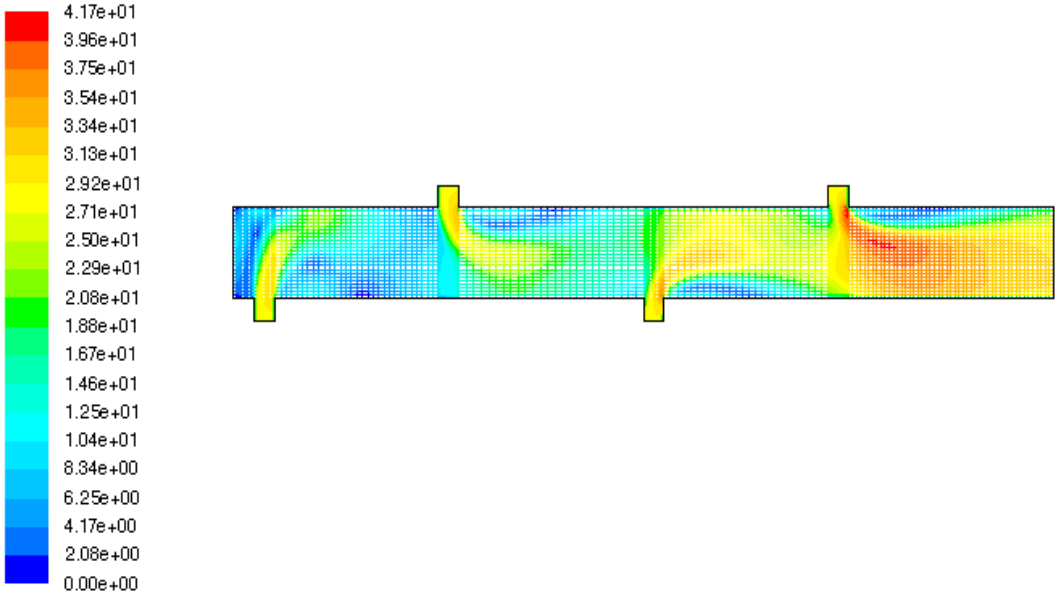

(a)

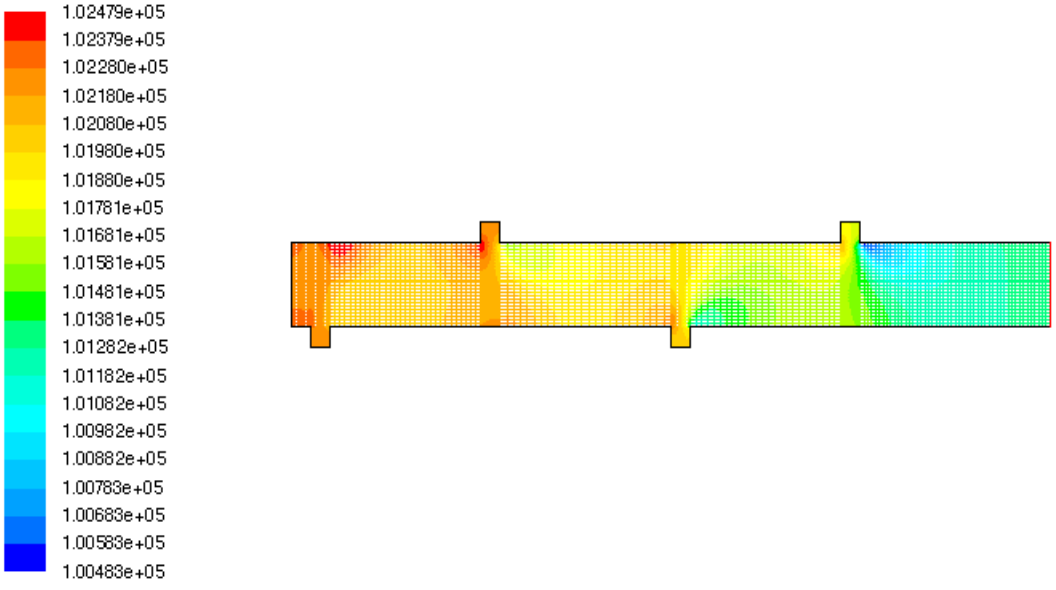

(b)

Figure 3.9 Velocity and Pressure Contours of Two-dimensional Model with Offset Inlets at *t* =0.01s (a) Case ii: 2-D velocity contours, b) Case ii: 2-D pressure contours.

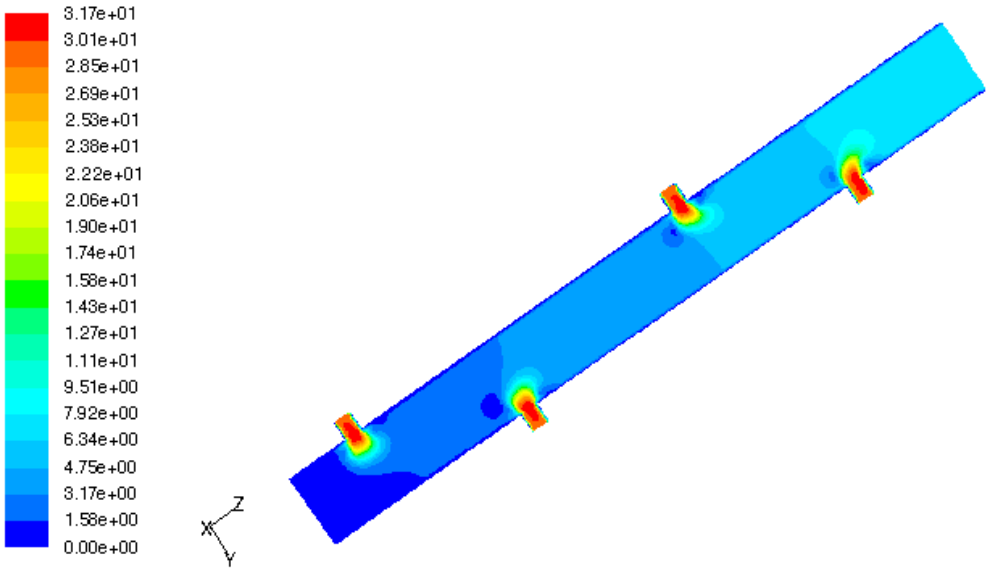

(a)

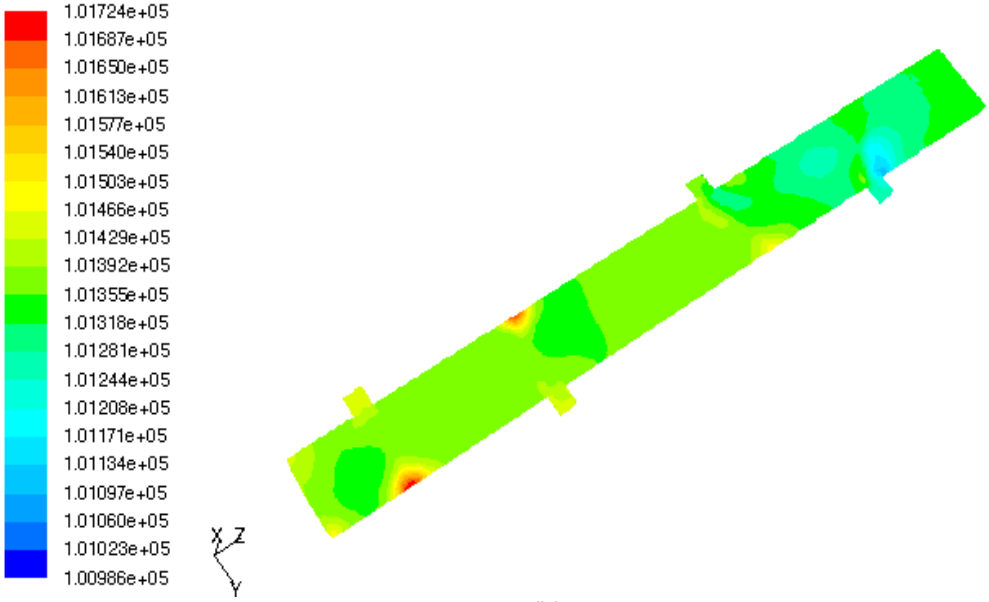

(b)

Figure 3.10 Isometric Views of Velocity and Pressure Contours at t =0.005 s (a) Case 2: 3-D velocity contours, (b) Case 2: 3-D pressure contours.

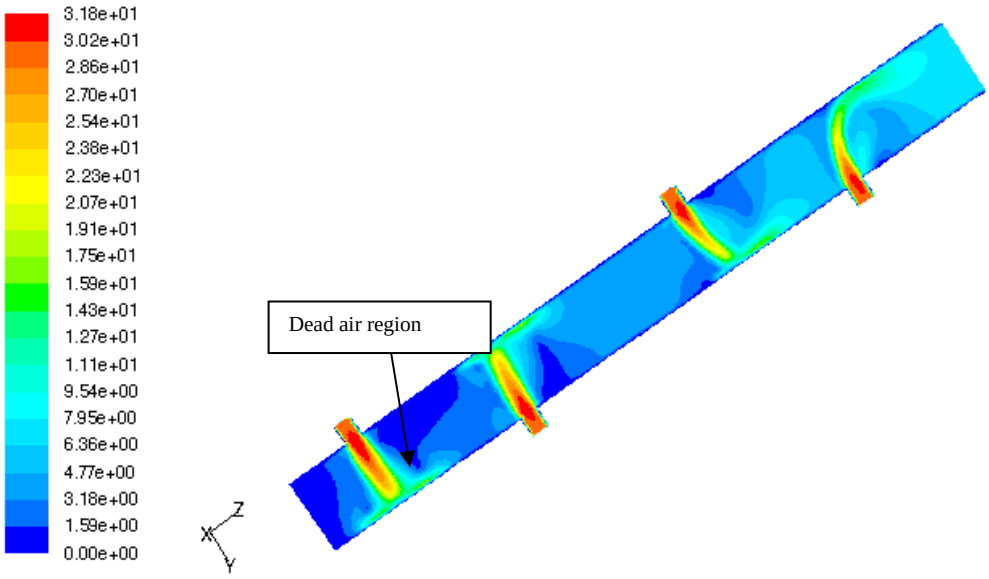

(a)

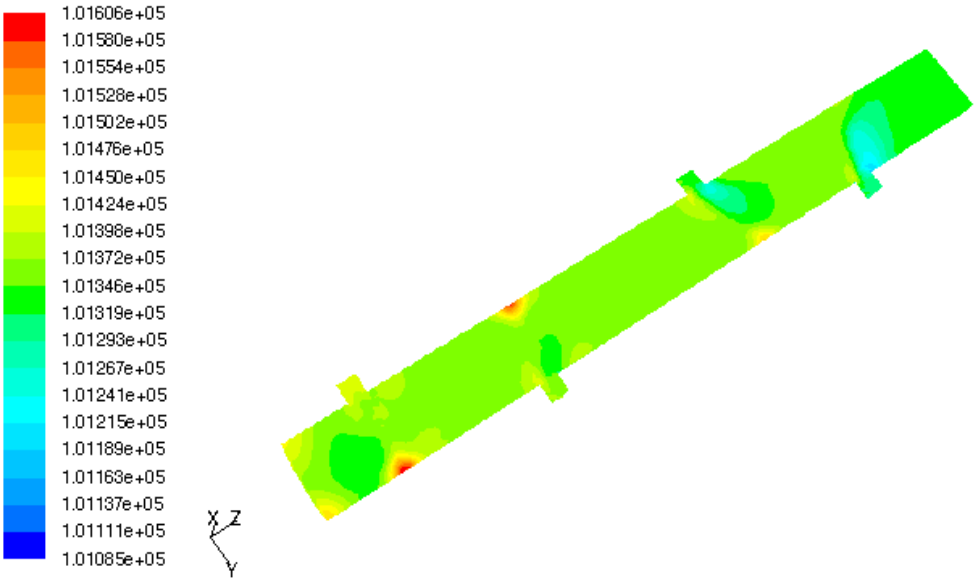

(b)

Figure 3.11 Isometric Views of Velocity and Pressure Contours at t =0.01 s (a) Case 2: 3-D velocity contours, (b) Case 2: 3-D pressure contours.

3.1.4 Case 3

In this model of opposite inlets, some dead air regions at closed end of the detonation tube are found. The blue colored area in velocity contours represents the dead air region. It is also possible to see from the velocity contours that the flow inside the tube is slower than that at the inlet and outlet. The velocity of the reactants mixture inside the detonation tube ranges from 0 to 33 m/s.

Figure 3.12 (a-b) shows the velocity and pressure contours of the two-dimensional model. Figures 3.13 (a-b) show the isometric views of the velocity and pressure contours at t =0.005 s and Figures 3.14 (a-b) show the isometric views of the pressure and velocity contours at t =0.013 s.

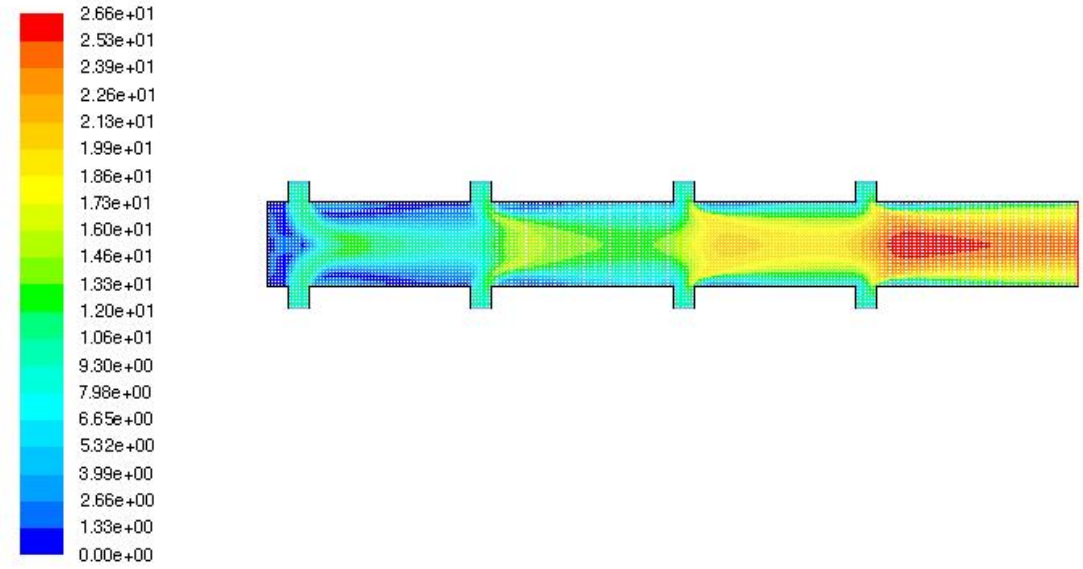

(a)

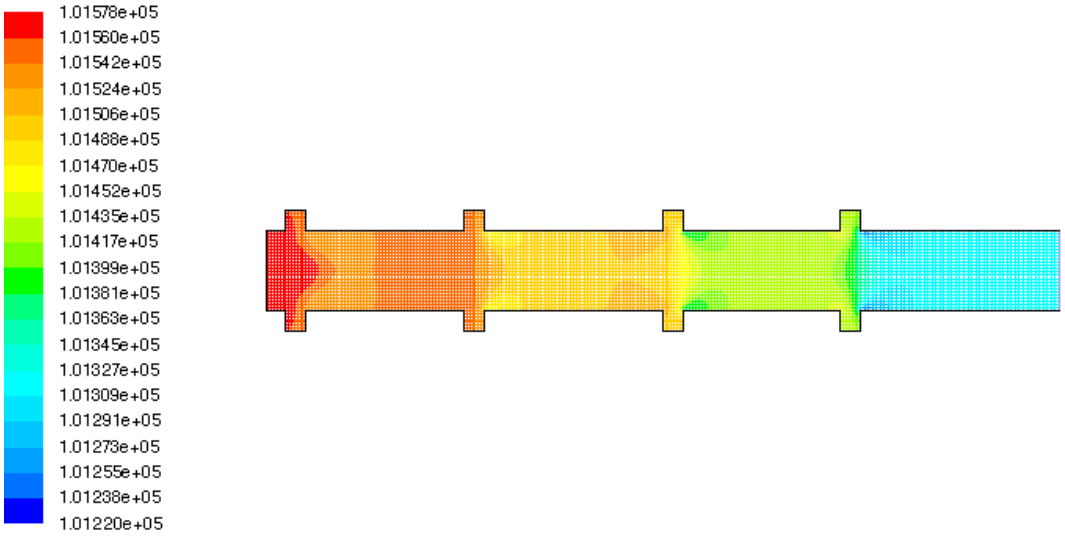

(b)

Figure 3.12 Velocity and Pressure Contours of Two-dimensional Model with Opposite Inlets at *t* =0.01 s a) Case iii: 2-D velocity contours, b) Case iii: 2-D pressure contours.

.

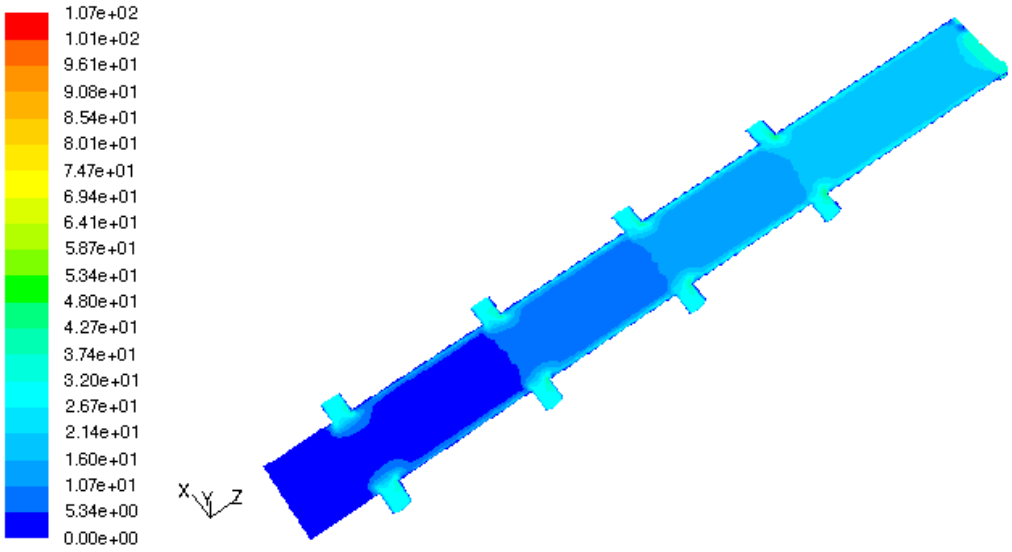

(a)

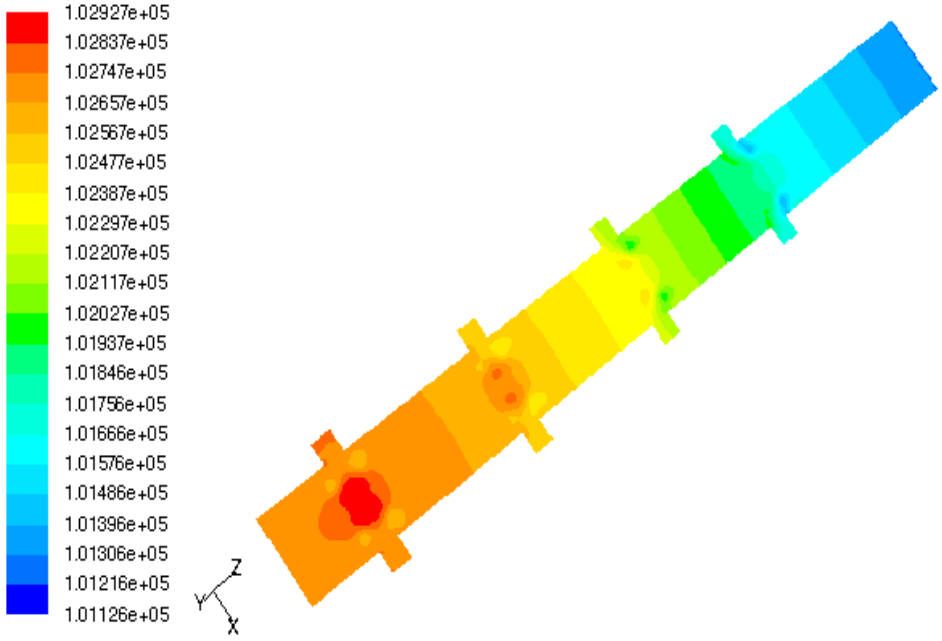

(b)

Figure 3.13 Isometric Views of Velocity and Pressure Contours at t =0.005 s (a) Case 3: 3-D velocity contours, (b) Case 3: 3-D pressure contours.

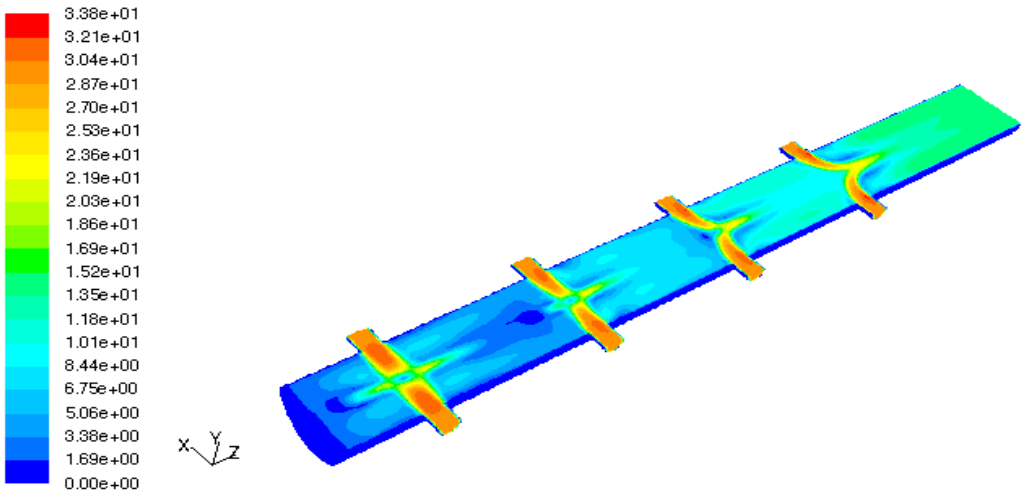

(a)

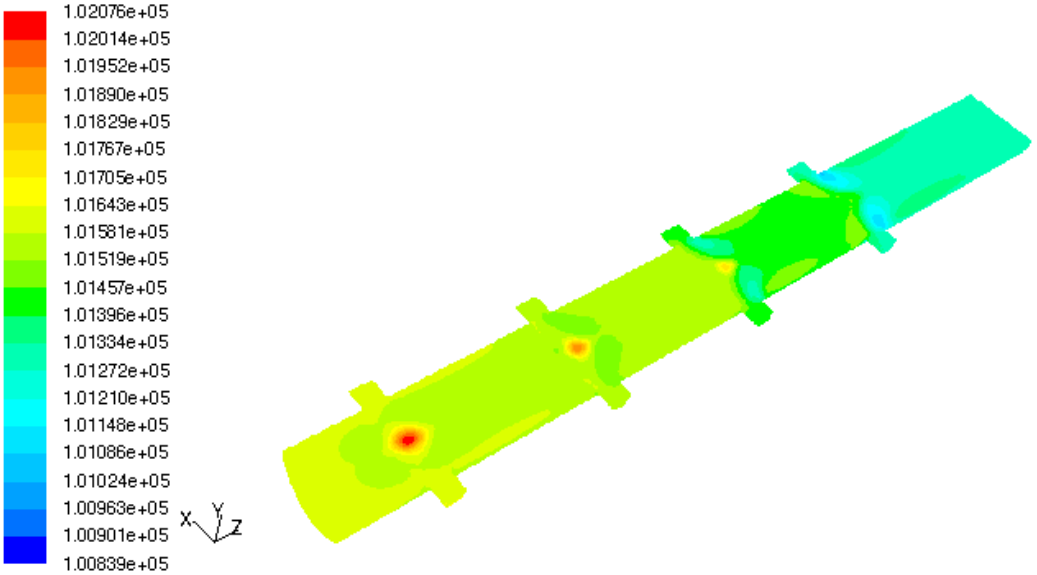

(b)

Figure 3.14 Isometric views of Velocity and Pressure contours at t =0.013 s (a) Case 3: 3-D velocity contours, (b) Case 3: 3-D pressure contour.

3.1.5 Case 4

The model was modified to reduce the dead air regions by adding an inlet at the closed end. The modified design gives the desired results but the problem of fuel wastage is raised. During the filling process of detonation tube, fuel enters from all nine inlets with the same velocity causing the area near the outlet of the tube to fill before the remaining tube is filled. This causes wastage of the reactants mixture. Figure 3.17 (a) shows that the flow of reactants was not uniform inside the detonation tube. The light red colored regions in the velocity contours represent the high velocity zones near the inlets. However, when compared with case 2 and 3 the dead air regions in this model are reduced.

Figure 3.15 (a-b) shows the velocity and pressure contours of the two-dimensional model with a inlet at the closed end. Figures 3.16 (a-b) show isometric views of the velocity and pressure contours at t =0.004 s and Figures 3.17 (a-b) show the isometric views of the pressure and velocity contours at t =0.013 s.

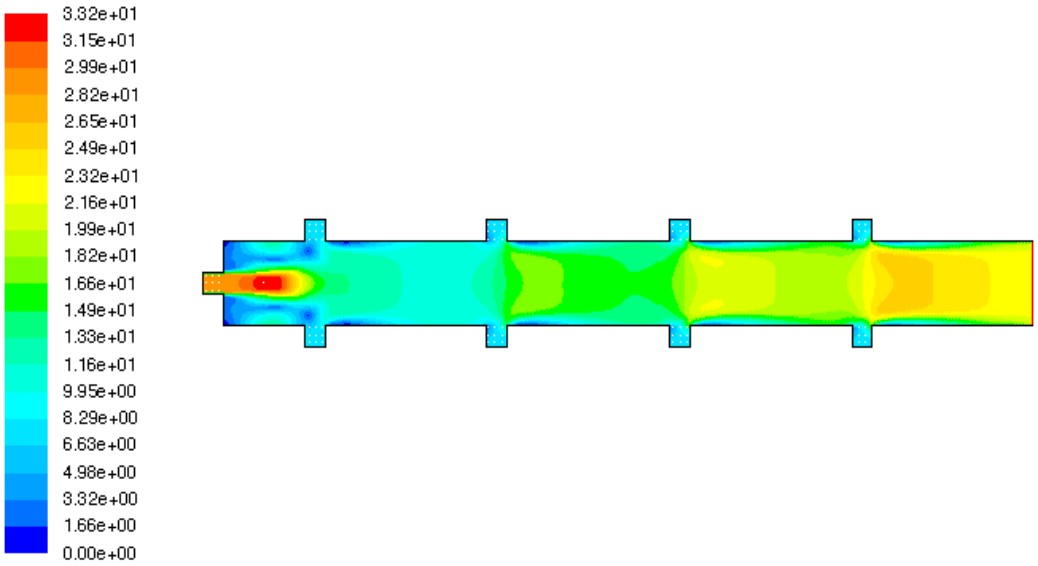

(a)

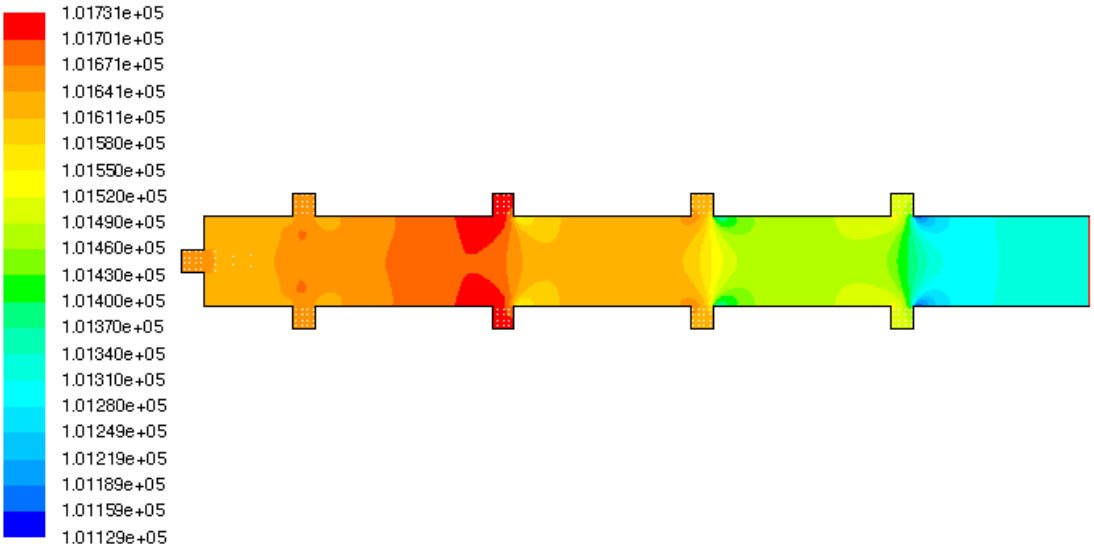

(b)

Figure 3.15 Velocity and Pressure Contours of Two-dimensional Model with an Inlet at Closed End t =0.01 s (a) Case iv: 2-D velocity contours, (b) Case iv: 2-D pressure contours.

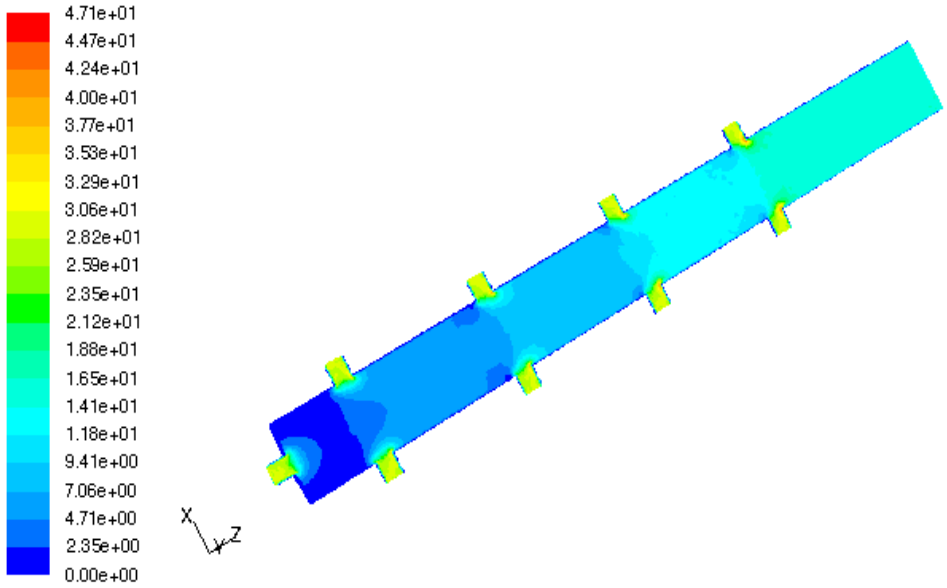

(a)

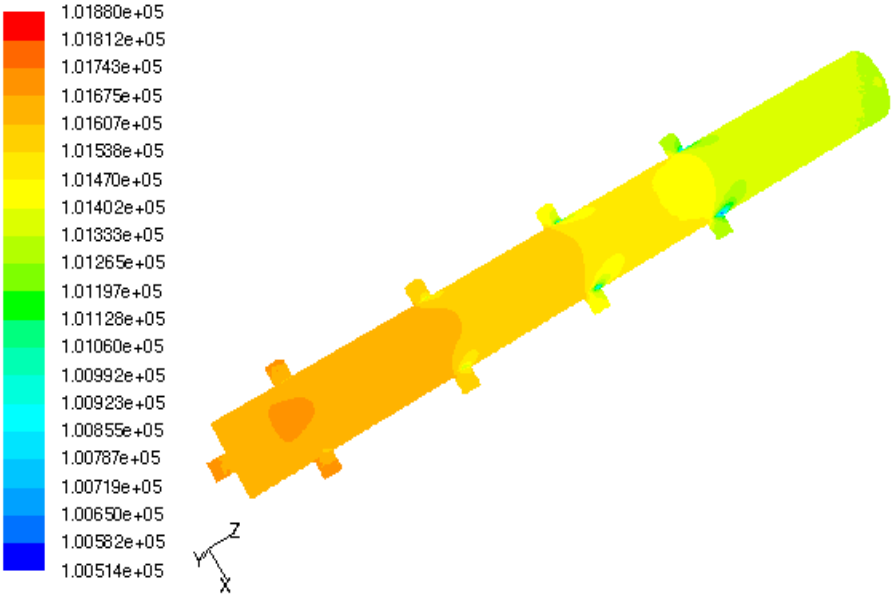

(b)

Figure 3.16 Isometric Views of Velocity and Pressure contours t =0.004 s (a) Case 4: 3-D velocity contours b) Case 4: 3-D pressure contours.

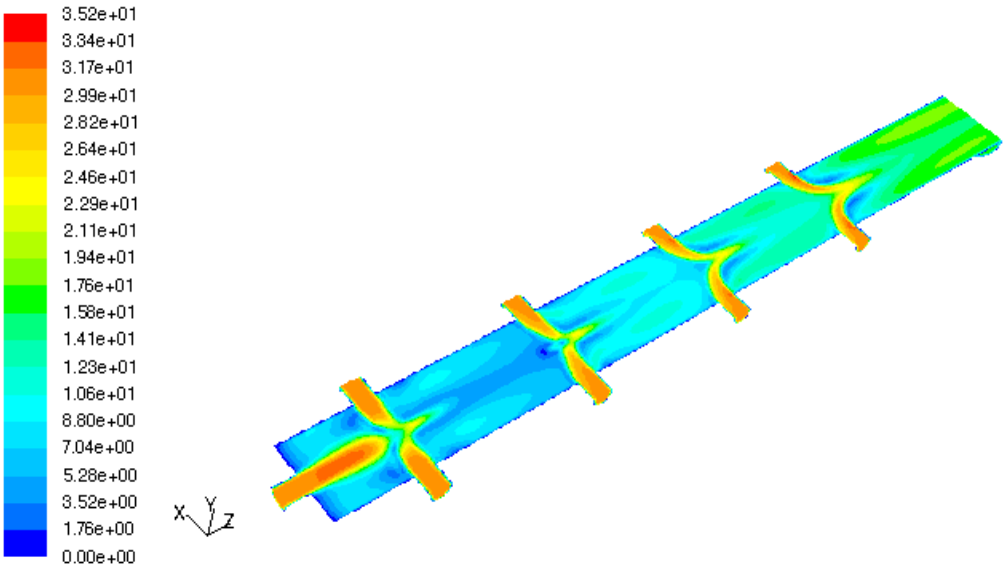

(a)

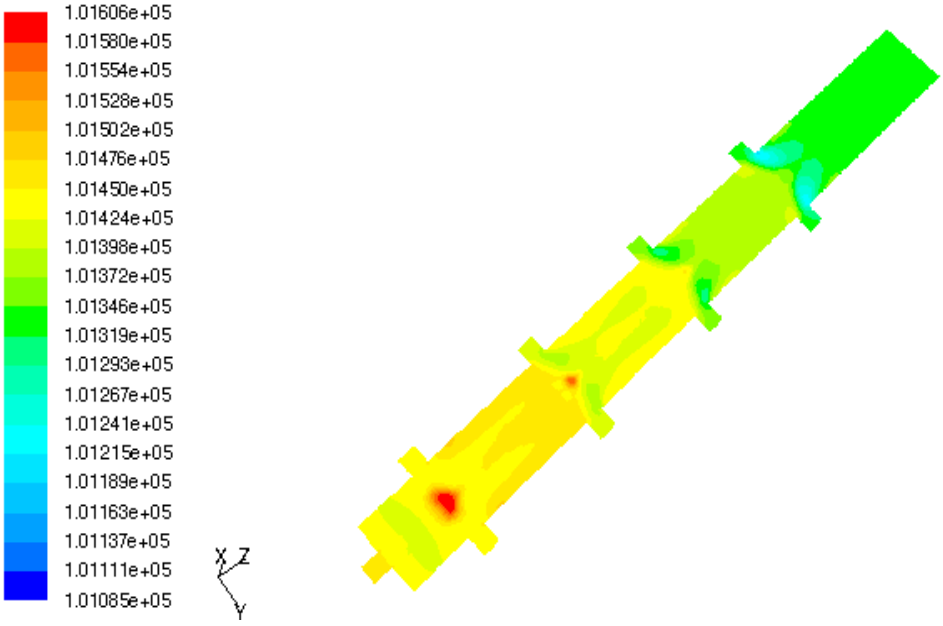

(b)

Figure 3.17 Isometric Views of Velocity and Pressure Contours at t =0.013 s (a) Case 4: 3-D velocity contours, (b) Case 4: 3-D pressure contours.

3.1.6 Case 5

The model was further modified by adding an orifice plate at the inlets in order to decrease the inlet velocity to avoid the wastage of the reactant mixtures and minimize dead air regions. Figure 3.18 shows the velocity and pressure contours of the two-dimensional model. The velocity and pressure contours at t =0.005 s and t =0.03 sare shown in Figures 3.19 (a-b) and 3.20 (a-b) respectively.

As noticed from the velocity contours, the flow in the detonation tube is relatively uniform and also if noticed closely, that the velocity is lower at the inlets of the detonation tube. From Figure 3.20 (a), it is clearly seen that the detonation tube is completely filled with the reactant. As the velocity inside the detonation tube is almost constant, the pressure variation is also very low as seen in Figures 3.19-3.20. The maximum velocity attained is 31 m/s. In Figure 3.20 (a), some red regions are spotted, these appear due to stagnation near the inlets. Stagnation occurs as the detonation tube gets completely filled with reactants. Due to the reduced flow rates with fewer ports, then the filling times in those cased will be longer. The time taken to fill the detonation tube with orifice pate at the inlets $t_{fill} = 0.03$ s. When compared with the previous models, an optimum solution is obtained in this model with orifice plates at the inlets.

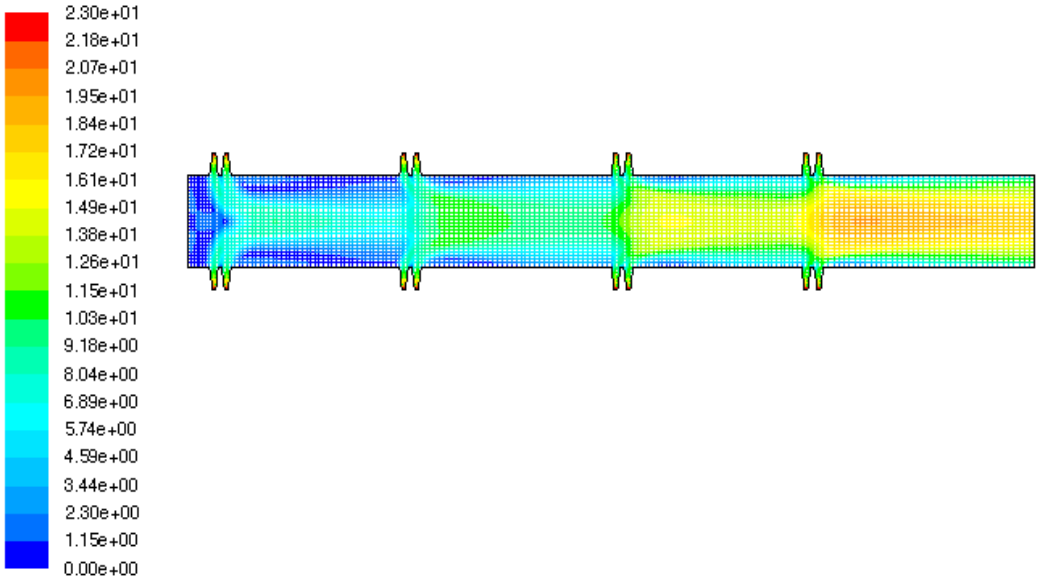

(a)

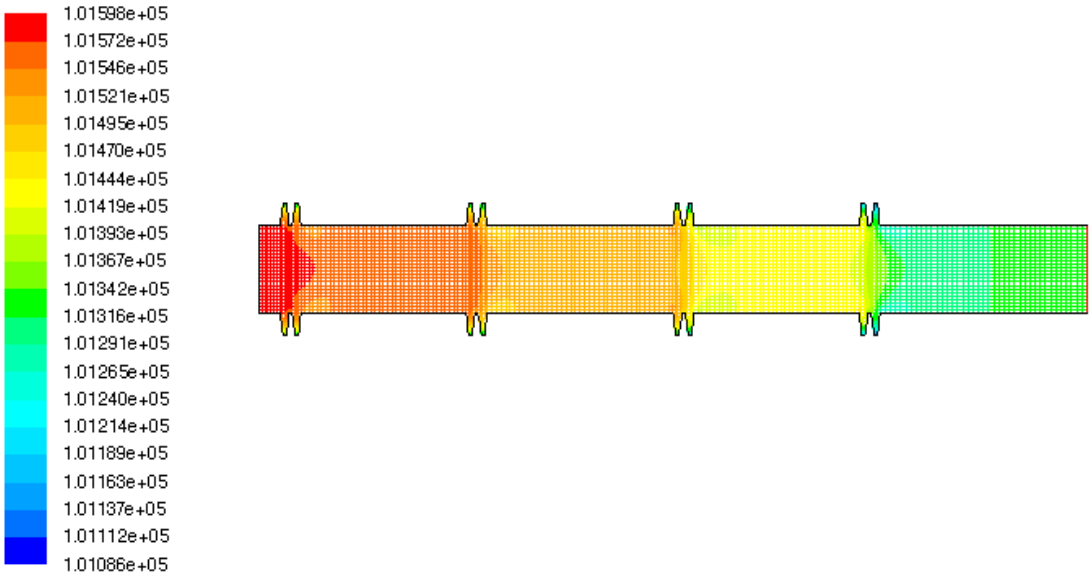

(b)

Figure 3.18 Velocity and Pressure Contours of Two-dimensional Model with an Orifice Plate at *t* =0.07 s a) Case v: 2-D velocity contours, b) Case v: 2-D pressure contours.

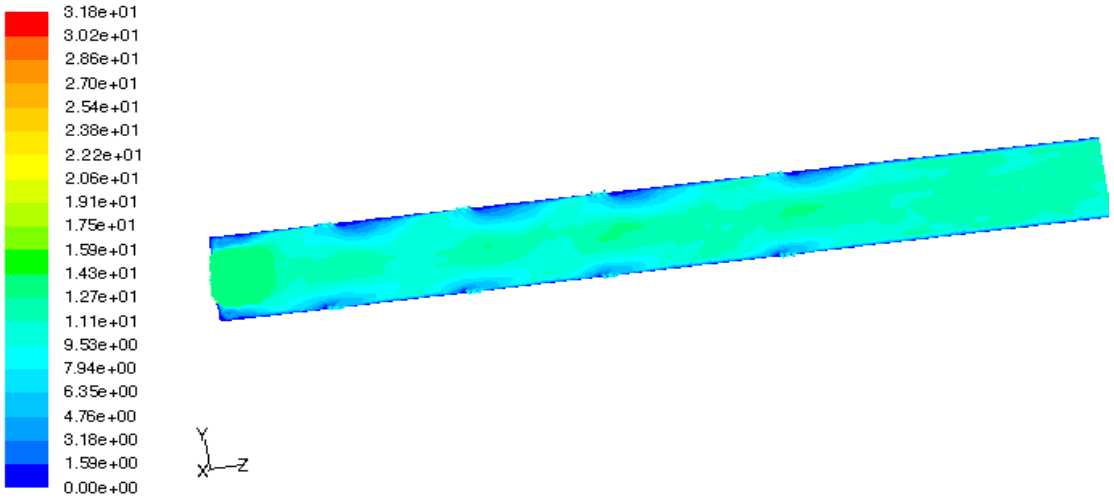

(a)

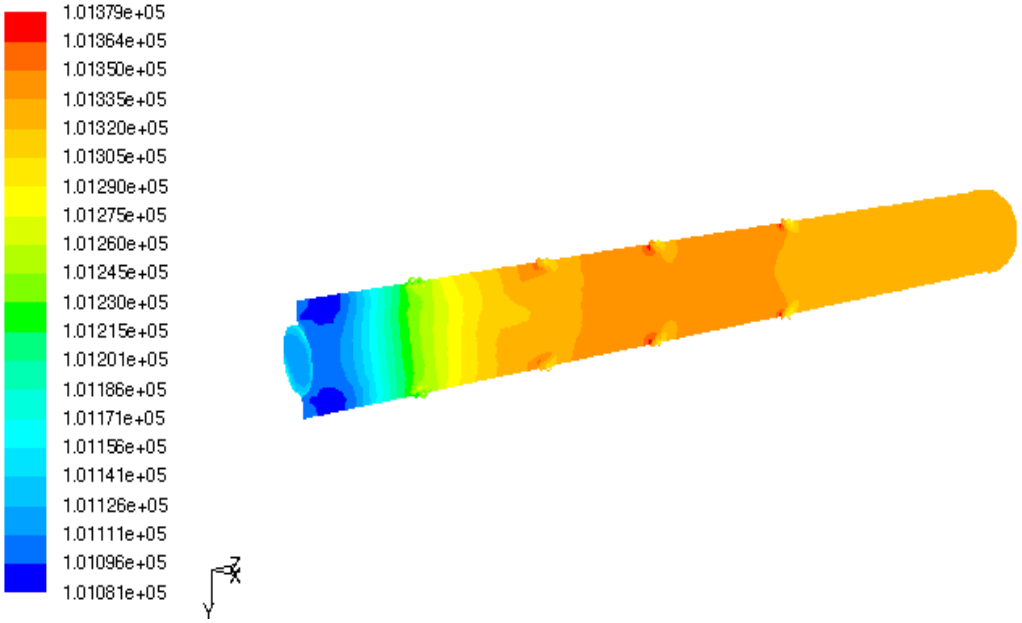

(b)

Figure 3.19 Isometric Views of Velocity and Pressure Contours at t =0.005 s (a) Case 5: 3-D velocity contours, (b) Case 5: 3-D pressure contours.

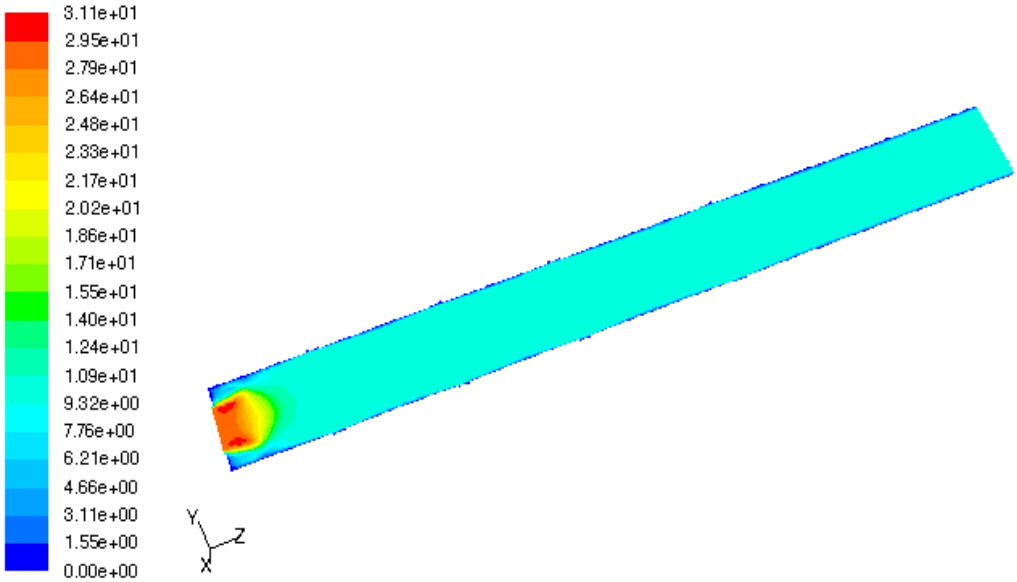

(a)

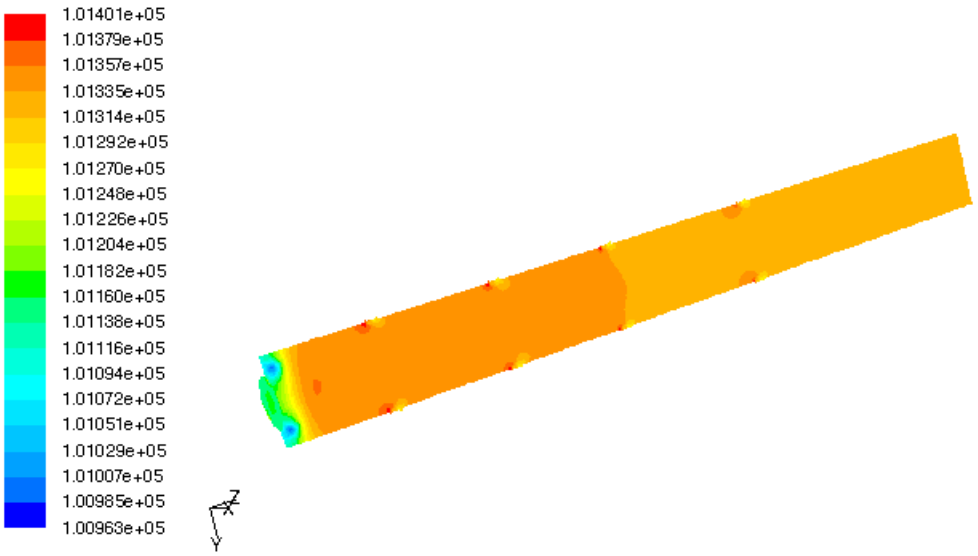

(b)

Figure 3.20 Isometric Views of Velocity and Pressure Contours at t =0.03 s a) Case 5: 3-D velocity contours, b) Case 5: 3-D pressure contours.

CHAPTER 4

CONCLUSIONS AND RECOMMENDATIONS

4.1 Conclusions

The tube filling process for a model pulse detonation engine was modeled using FLUENT™. Simulation of the filling process was accomplished using five different inlet configurations proposed both two-dimensionally and three-dimensionally. Comparison of these five configurations revealed that the inlet configuration with orifice plate provides optimum results with desired velocity and pressure profiles as per design requirements. This configuration also ensures that the detonation tube is well filled with reactants at a uniform velocity with small dead air regions. When compared with existing designs, with only one inlet at the closed end ($t_{fill} = 0.2$ s), the filling time is reduced as this model has nine inlets ($t_{fill} = 0.03$ s).

4.2 Recommendations and Future Work

Further research is needed to simulate a multiphase flow using the Volume of Fluid (VOF) model in FLUENT™. Using the VOF model, we can simulate droplet or slug flow. This will enable more precise results. Moreover, we can simulate the complete cycle analysis of pulsed detonation engine.

Further investigations may be conducted to investigate the particle motion of reactants entering the detonation tube using spray modeling technique which is included in FLUENT™.

Future work may include experimental results. Once experimental processes have been carried out, the experimental results will be utilized for comparison to the model predictions such that the overall accuracy of CFD simulation can be determined.

APPENDIX A

POST-PROCESSING IN FLUENT™

The final post processing was carried out in FLUENT™, with the model set up for a transient analysis.

1. The mesh file was imported from GAMBIT™ to FLUENT™ for grid check.

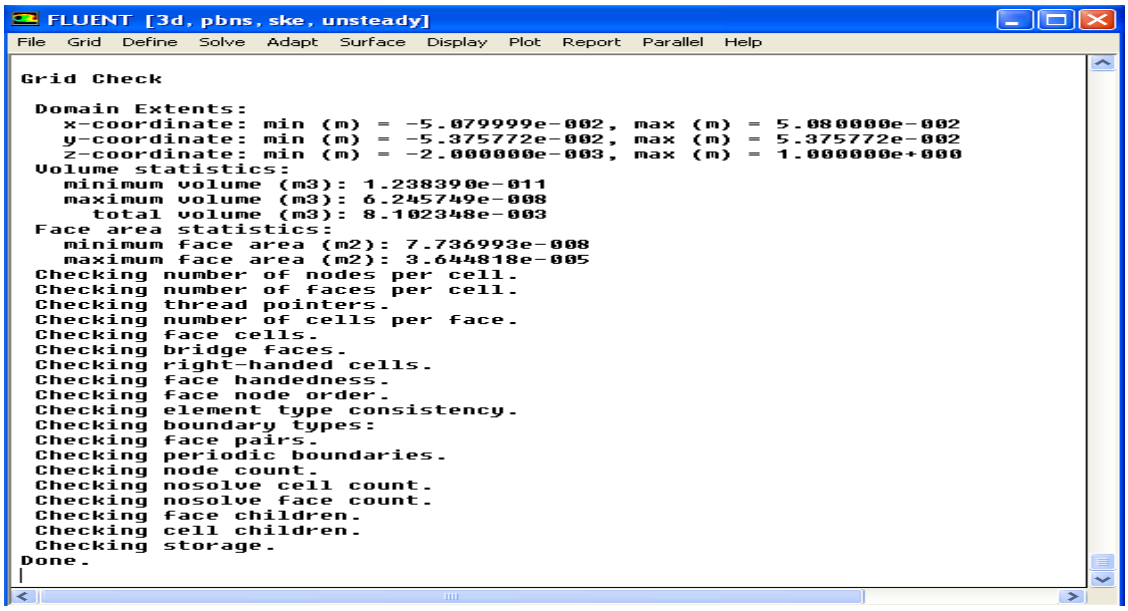

Figure A1 FLUENT Command Prompt Showing Grid Check.

2. Define the model

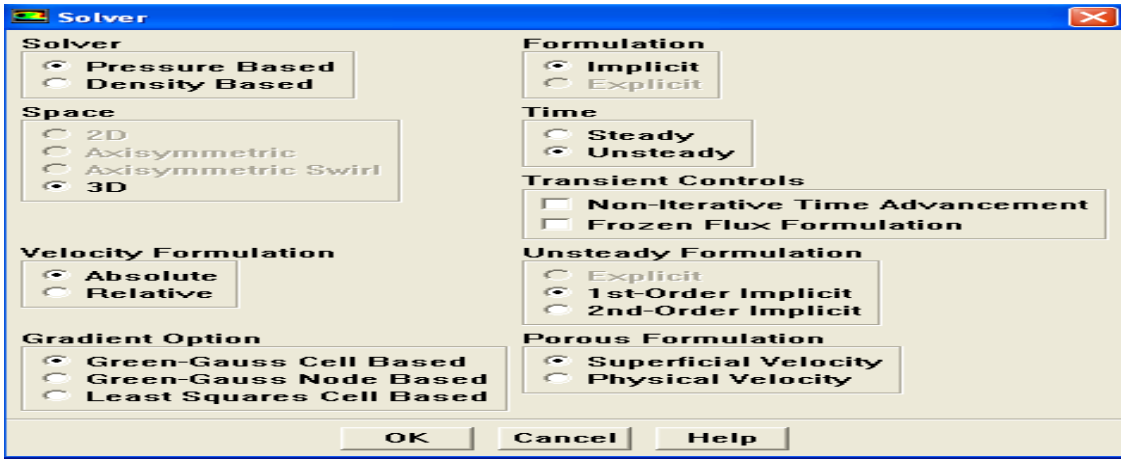

Figure A2 FLUENT Command Prompt Showing Solver Conditions.

3. The energy equation was selected. (*Define – Modes- Energy*)

4. The standard κ−ε turbulence model was selected (*Define –Models –Viscous*)

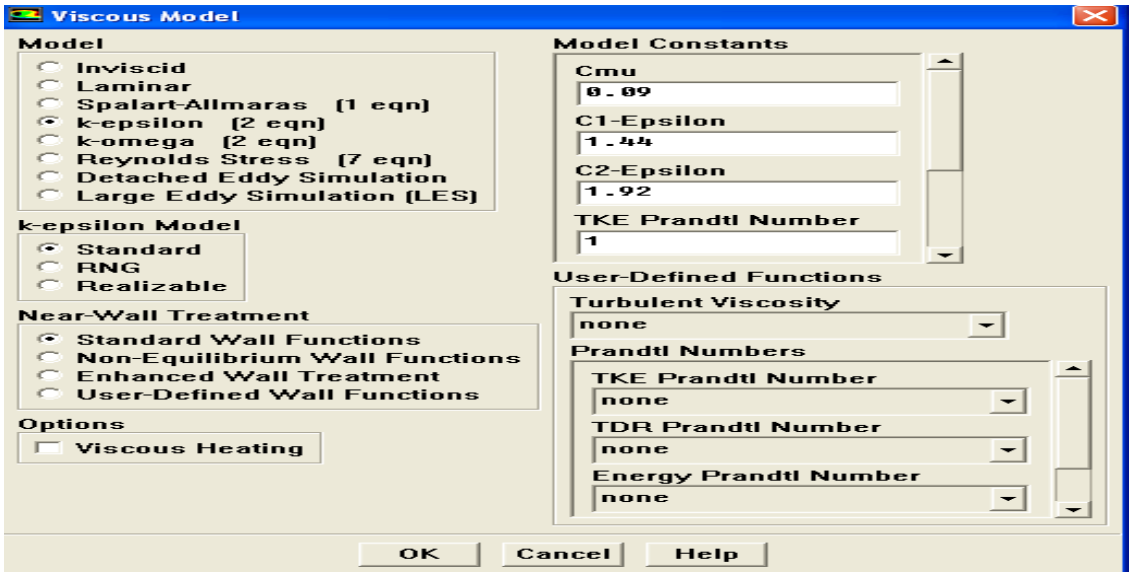

Figure A3 FLUENT Command Prompt Showing Turbulence Model Conditions

5. Define the fluid.

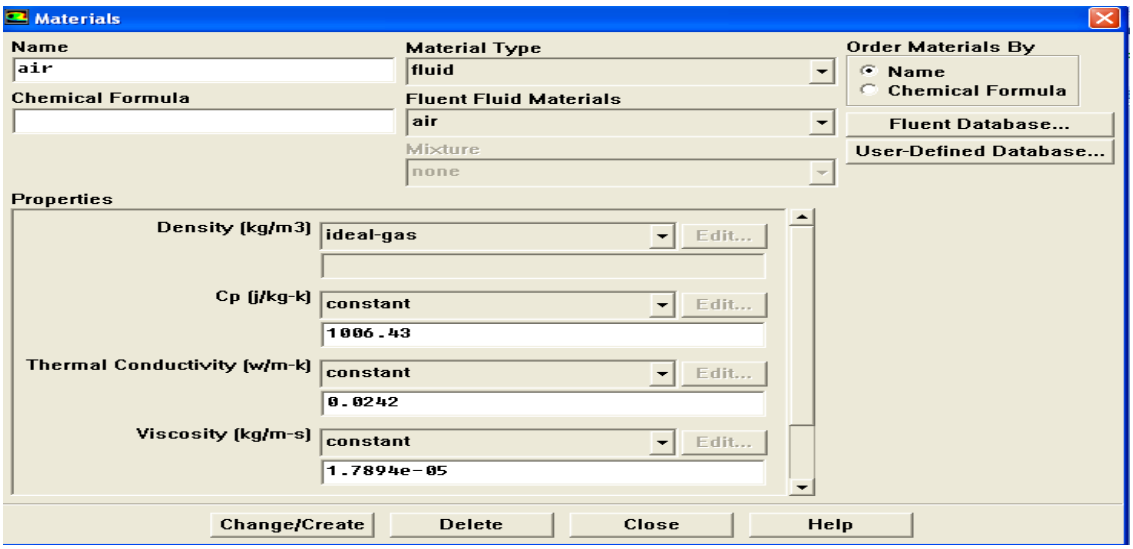

Figure A5 FLUENT Command Prompt Showing Fluid Properties.

6. Define boundary conditions. *(Define – Boundary conditions)*

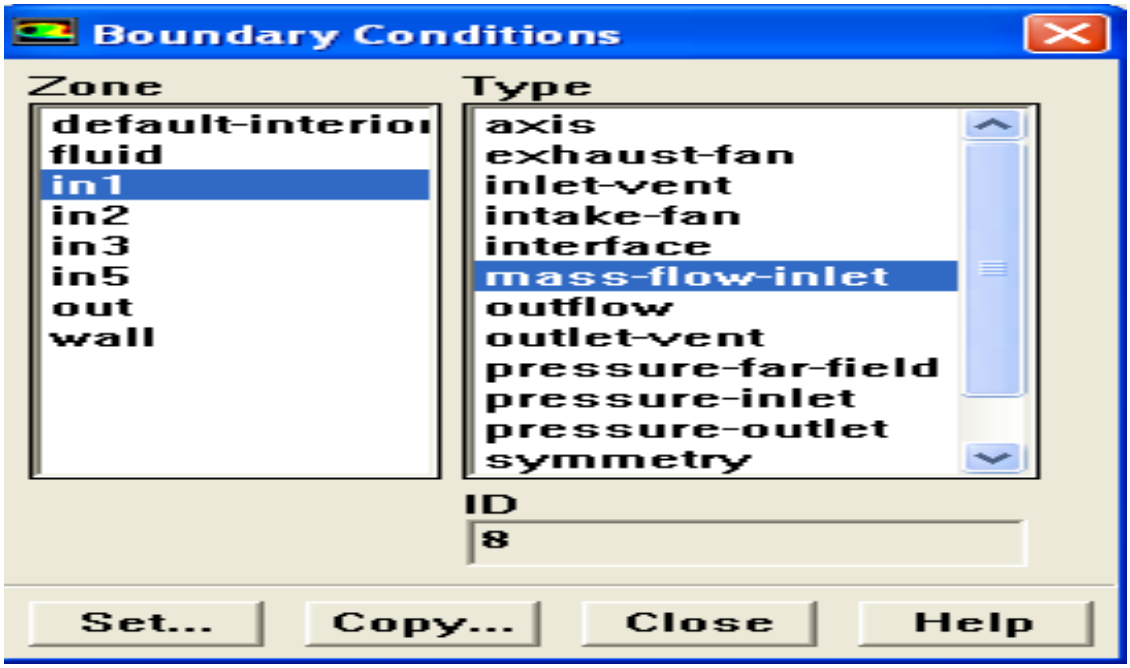

Figure A6 FLUENT Command Prompt Showing Inlet Boundary Conditions.

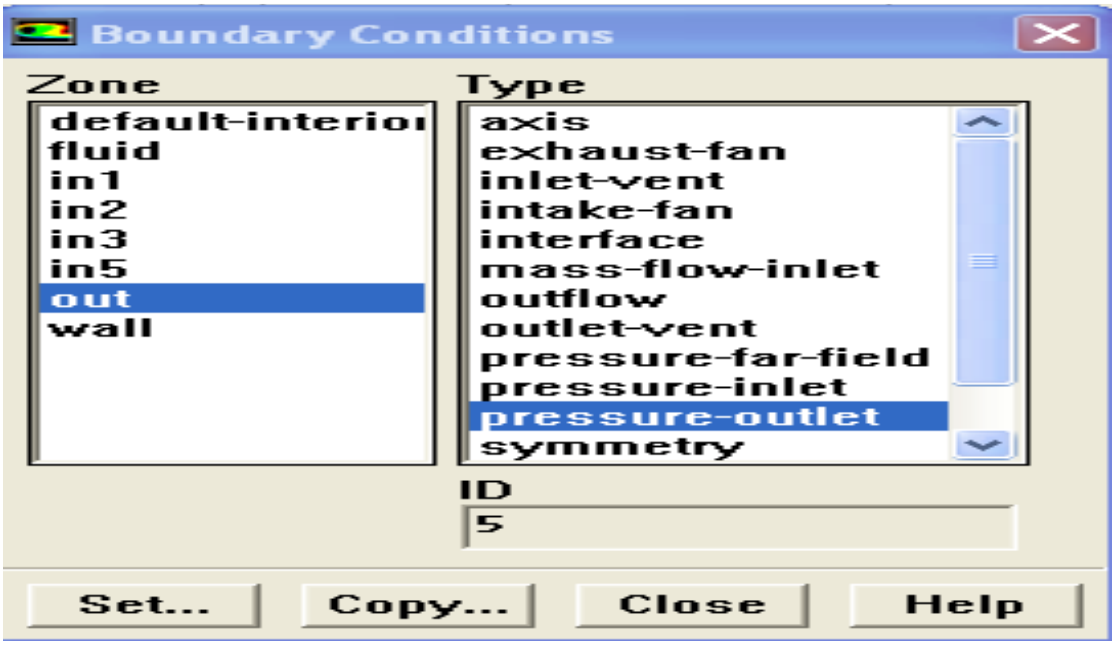

Figure A7 FLUENT Command Prompt Showing Outlet Boundary Conditions.

7. Define solution method. *(Solve – Controls-Solution)*

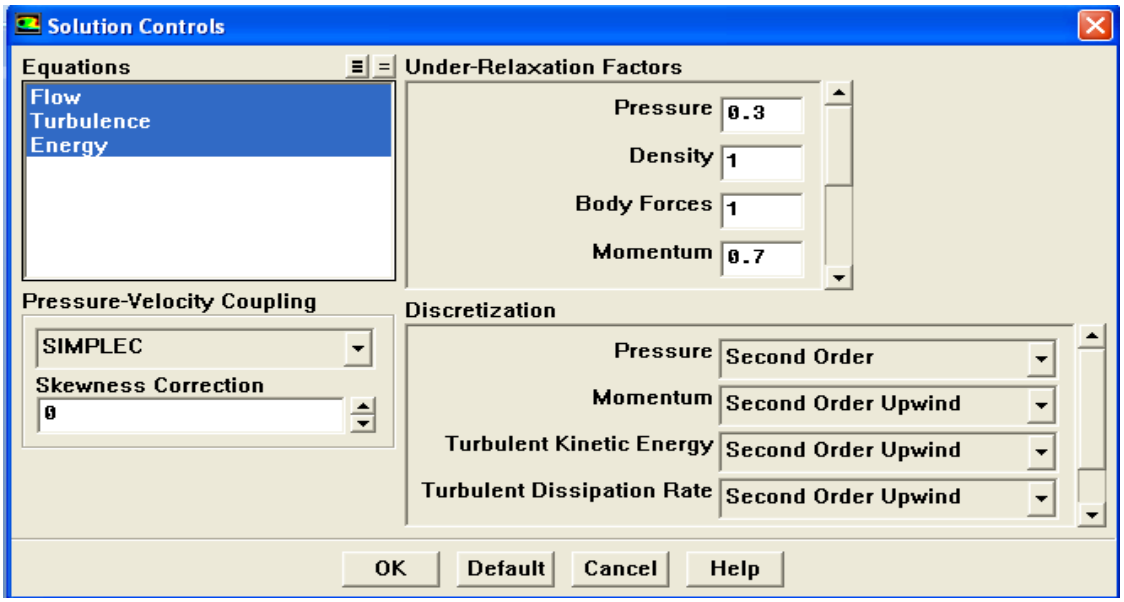

Figure A8 FLUENT Command Prompt Showing the Solution Method.

.

REFERENCES

[1] Hill, P. and Peterson, C., *Mechanics and Thermodynamics of Propulsion*, 2nd ed., Addison Wesley, Massachusetts, 1992.

[2] Bussing T.,and Pappas, G.," An Introduction to Pulse Detonation Engines," AIAA paper 94-0263, January 1994.

[3] Kialasanath, K.,"Recent Developments on the Research on Pulse Detonation Engines," AIAA Journal, Vol. 41, No.2, 2003.

[4] Panicker, Philip K., "The Development and Testing of Pulsed Detonation Engine Ground Demonstrators," Doctoral Dissertation, Department of Mechanical and Aerospace Engineering, The University of Texas at Arlington, Arlington, TX, 2008.

[5] Allgood, Daniel Clay. An Experimental and Computational Study of Pulse Detonation Engines. Degree: PhD, Engineering: Aerospace Engineering, 2004, University of Cincinnati.

[6] Google Patent Office, URL: www.google.com/patents

[7]United States Patent and Trademark Office, URL: http://www.uspto.gov/patft/index.html.

[8] European Patent Office, URL: htpp://www.epo.org/.

[9] Heiser, W. h. and Pratt, D.T., *Hypersonic Airbreathing Propulsion*, AIAA Education Series, Washington D.C., 1994, ODWE: 545-551.

[10] B.R Munson, D.F. Young and T.H. Okiishi, *Fundamentals of fluid mechanics,* 4th ed*,* John Wiely & Sons., New York, 2002.

[11] FLUENT 6.2 User's Guide, Fluent Inc., 2005

12 Fluent Inc., *Gambit 2.4 User's Manual*, Lebanon, NH, USA (2006)

13 Fluent Inc., *Fluent 6.3 User's Manual*, Lebanon, NH, USA (2006)

BIOGRAPHICAL INFORMATION

Suneel, an aspiring, inquisitive and a hardworking student, was born in land of varied culture and integrity-INDIA on June19th1985. He has always stood in the first 5% in the class. He pursued his Bachelor's degree in Mechanical engineering from Jawaharlal Nehru technological university in 2006. He has an experience as a design engineer for a year. His interest in the aerospace engineering made him opt it for his master's degree from spring 2008 at University of Texas at Arlington, Texas. His field of interest was always designing and this zeal made him choose the field of CFD and used the same in research of PDE and `achieved his Master's degree in Aerospace engineering.